Journal of Asian Earth Sciences 35 (2009) 445–458

Contents lists available at ScienceDirect

Journal of Asian Earth Sciences

journal homepage: www.elsevier.com/locate/jaes

Zircon U–Pb age, geochemistry and Sr–Nd–Pb isotopic compositions of adakitic volcanic rocks from Jiaodong, Shandong Province, Eastern China: Constraints on petrogenesis and implications

Shen Liu [a,b,c,*], Ruizhong Hu [a], Shan Gao [b], Caixia Feng [a], Bobin Yu [d], Youqiang Qi [a], Tao Wang [a], Guangying Feng [a], Ian M. Coulson [e]

[a] *State Key Laboratory of Ore Deposit Geochemistry, Institute of Geochemistry, Chinese Academy of Sciences, Guiyang 550002, China*
[b] *State Key Laboratory of Geological Processes and Mineral Resources, China University of Geosciences, Wuhan 430074, China*
[c] *State Key Laboratory of Continental Dynamics, Northwest University, Xi'an 710069, China*
[d] *No.7 Brigade of China Armed Police, Shandong Yantai 264004, China*
[e] *Solid Earth Studies Laboratory, Department of Geology, University of Regina, Regina, Saskatchewan S4S 0A2, Canada*

ARTICLE INFO

Article history:
Received 28 June 2008
Received in revised form 12 February 2009
Accepted 26 February 2009

Keywords:
Adakitic volcanic rocks
Lower continental crust
Foundering
Jiaodong
North China Craton (NCC)

ABSTRACT

A zircon U–Pb age of adakitic rocks from Jiaodong, the Shandong Province, indicates that the volcanic rocks erupted at 123.6 ± 0.8 Ma. The volcanic rocks are composed only of trachyandesite with SiO_2 contents ranging from 59 to 62 wt.% and Al_2O_3 contents from 14 to 16 wt.%. Their K_2O contents range from 3.1 to 3.9 wt.% and those of Na_2O from 4.2 to 4.9 wt.%, indicating that these rocks belong to the alkaline K-rich series. These rocks are characterized by enrichment in light rare earth elements (LREE) and depletion in heavy rare earth elements (HREE). They show strongly positive Ba anomalies and negative Nb, Ta, and Ti anomalies. The trachyandesites have high concentration of Sr, ranging from 919 to 1376 ppm, and low Yb (0.92–1.16 ppm) and Y contents (13.3–15.0 ppm), resulting in high Sr/Y (65–98) and La/Yb ratios (38–51), all of which are characteristics of adakites defined by Defant and Drummond [Defant, M.J., and Drummond, M.S., 1990. Derivation of some modern arc magmas by melting of young subducted lithosphere. Nature 347, 662–665]. Isotopic compositions have high Sr and Pb ratios ($^{87}Sr/^{86}Sr = 0.7097–0.7099$; $^{208}Pb/^{204}Pb = 37.71–38.30$; $^{207}Pb/^{204}Pb = 15.34–15.54$; $^{206}Pb/^{204}Pb = 16.95–17.19$), but low Nd ($^{143}Nd/^{144}Nd = 0.51150–0.51153$; $\varepsilon_{Nd}(t) = -18.5$ to -19.1). These geochemical features suggest a mafic, lower crust magma source. High Sr/Y and La/Yb ratios and negative Nb and Ti anomalies of the adakitic rocks suggest that garnet and amphibole were stable as two residual phases during partial melting, implying that the crustal thickness exceeded 40 km in the Early Cretaceous. The present thickness of the crust in the Jiaodong area is only ~32 km, and therefore the crust appears to have been thinned by at least 8–10 km since Early Cretaceous times. The high MgO (2.7–3.3 wt.%), Cr (93–274 ppm), and Ni (60–115 ppm) contents and high Mg# (46–52) values in the adakitic rocks favours interaction between the pristine melts and mantle peridotite prior to eruption.

1. Introduction

Adakites (Defant and Drummond, 1990) were first described at convergent plate margins and are thought to be the products of melting relatively young (<25 Ma) and hot oceanic crust (Kay, 1978) in subduction-zones. Such rocks are characterized by high Al, Na, and Sr contents, high Sr/Y and La/Yb ratios, and low Y and Yb contents; these characteristics are consistent with an origin by partial melting of hydrated mafic source rocks in the form of eclogite or garnet amphibolite (Rapp et al., 1991; Martin, 1998). However, some rocks with adakitic compositional features may have a different origin, such as: (1) assimilation-fractional crystallization (AFC) processes (e.g., Castillo et al., 1999; Macpherson et al., 2006), (2) melting of mantle peridotite under hydrous conditions (Stern and Hanson, 1991), or (3) partial melting of thickened lower crust (Atherton and Petford, 1993; Muir et al., 1995; Petford and Atherton, 1996; Johnson et al.,1997; Arculus et al., 1999; Zhang et al., 2001; Chung et al., 2003; Xiong et al., 2003; Hou et al., 2004; Wang et al., 2005; Guo et al., 2006) or delaminated mafic lower crust (e.g., Kay and Kay, 1993; Defant et al., 2002; Xu et al., 2002; Gao et al., 2004; Wang et al., 2004, 2006a,b; Guo et al., 2006; Lai et al., 2007; Liu et al., 2008a,c). Furthermore, experimental studies (Rapp and Watson, 1995; Rapp et al., 1999) have

---

* Corresponding author. Address: State Key Laboratory of Ore Deposit Geochemistry, Institute of Geochemistry, Chinese Academy of Sciences, Guiyang 550002, China. Tel.: +86 851 5895187; fax: +86 851 5891664.
E-mail address: liushen@vip.gyig.ac.cn (S. Liu).

1367-9120/$ - see front matter © 2009 Elsevier Ltd. All rights reserved.
doi:10.1016/j.jseaes.2009.02.008

shown that mafic materials can melt to produce an adakitic melt at pressures equivalent to a crustal thickness of >40 km (i.e., ~1.2 GPa). Generation of non-subduction related adakitic magmas is commonly linked with crustal thickening and eclogitization of the lowermost crust (Guo et al., 2006). Therefore, adakites can also be produced by melting of mafic lower crust in non-subduction settings, such as in collisional zones (e.g. Chung et al. 2003; Hou et al, 2004; Guo et al., 2006; Wang et al., 2007; Zi et al., 2007), intracontinental settings (Xu et al. 2002; Wang et al., 2005, 2006; Lai et al., 2007; Liu et al., 2008a,c) and active continental margins (Atherton and Petford, 1993; Petford and Atherton, 1996; Kay and Kay, 2002). Moreover, the investigation of non-subduction-related adakites can provide important constraints on crustal growth and its evolution throughout Earth history.

It is generally accepted that the North China Craton (NCC) lost its lithospheric keel (>100 km) between the Late Jurassic and Early Cretaceous (Menzies et al., 1993a,b; Griffin et al., 1998; Xu et al., 2000; Xu, 2001; Gao et al., 2002; Wu et al., 2003; Wilde et al., 2003; Zhang et al., 2004), accordingly, the NCC is an ideal place to evaluate the hypothesis of lower crust foundering (Gao et al., 2004). However, the exact timing of the lithospheric destruction beneath the NCC is poorly constrained. A number of controversial models have been proposed for the lithosphere thinning beneath NCC; these include foundering, extension or thermal/chemical erosion of the deep lithosphere due to upwelling asthenosphere (Menzies et al., 1993a,b; Griffin et al., 1998; Zheng and Lu, 1999; Lu et al., 2000; Xu, 2001; Gao et al., 2002, 2004; Rudnick et al., 2004; Wu et al., 2003, 2005, 2006; Menzies et al., 2007). The limited effect of tectonic extension on the lithosphere thickness beneath NCC has been explored by a numerical approach (Lin et al., 2004). In addition, thermo-chemical erosion of the lithospheric mantle by upwelling asthenosphere (Menzies et al., 1993a,b, 2007; Griffin et al., 1998) cannot explain the production of adakitic magma from foundered NCC crust prior to basaltic magmatism (Gao et al., 2004; Liu et al., 2008c). By contrast, foundering of lithosphere (mantle and lower crust) might be a plausible mechanism to account for the lithosphere thinning underneath NCC.

Eclogitization of the lowermost crust results in a mass density that is higher than that of lithospheric mantle peridotite by some 0.2–0.4 g cm^{-3} (Rudnick and Fountain, 1995). Hence, eclogite can be recycled into the mantle by foundering (Kay and Kay, 1993; Jull and Kelemen, 2001; Gao et al., 2004). Which has been confirmed beneath the NCC based on a study of the adakitic volcanic rocks from Liaoning (Gao et al., 2004), western Shandong (Luxi) (Liu et al., 2008c) and Xuzhou-Suzhou (Xu et al., 2006) located within the southeastern portion of the NCC. Nevertheless, in order to assess the validity of the model for lithosphere thinning beneath NCC, additional evidence for lithosphere foundering occurring within other areas of the NCC is needed. Our study deals with a new adakite locality within the eastern NCC and presents new zircon geochronology, geochemical, and Sr–Nd–Pb isotopic data to provide further support for the foundering of mafic lower continental crust within the NCC.

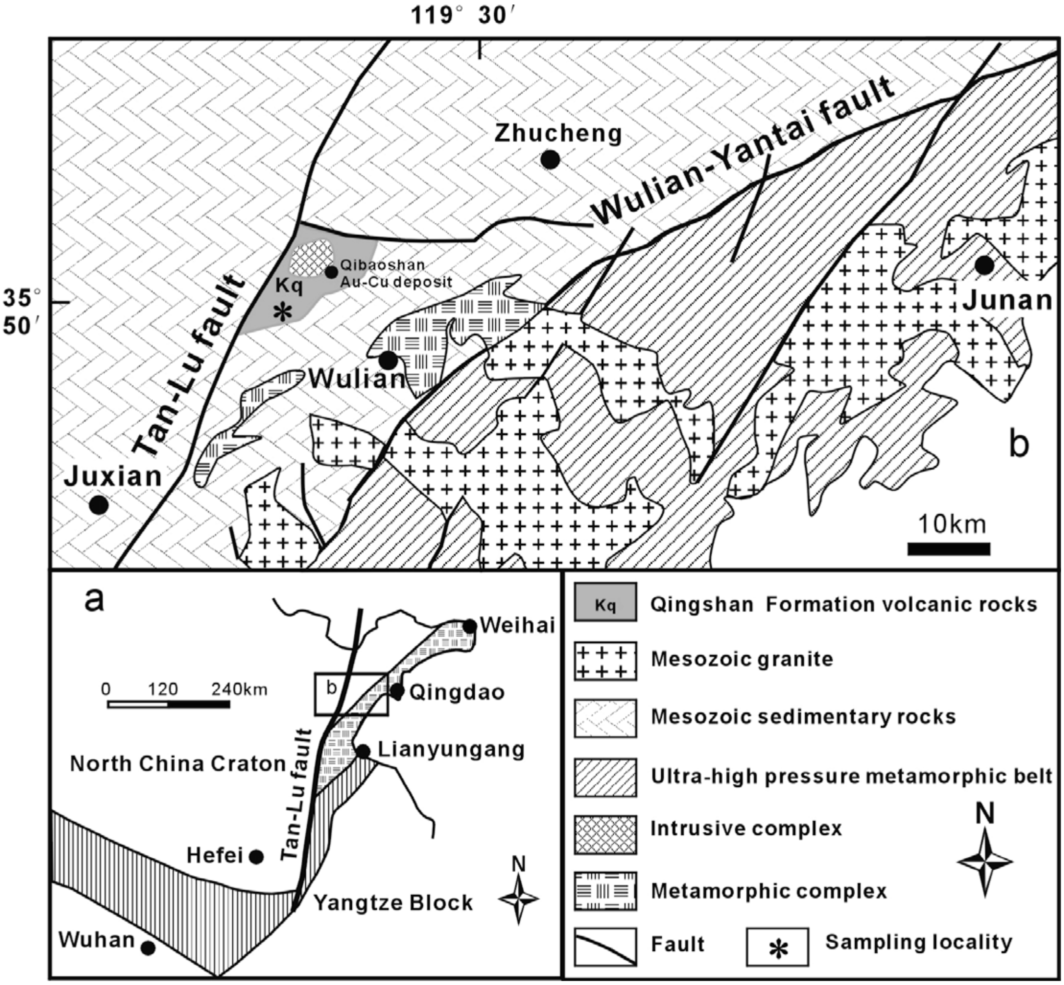

Fig. 1. (a) Simplified tectonic map showing the NCC, Yangtze Block, and Dabie-Sulu orogenic belt (modified after Zhou et al., 2003). (b) Geological sketch map of Mesozoic igneous rocks in the Sulu orogenic belt and the adakitic lavas in the eastern NCC (modified after Zhou et al., 2003).

2. Geological background and petrology

The eastern block of the NCC in Shandong Province is divided into two parts by the Tanlu fault, with Jiaodong to the east and Luxi to the west. In addition, the Jiaodong and South China Block (SCB) are detached from the Wulian-Yantai fault (WYF) (Fig. 1a). The study area is located in Jiaodong (Wulian region) in the eastern NCC, adjacent to the Sulu belt and Tanlu fault (Fig. 1a and b), where the large volume, Qingshan Formation volcanic and intrusive complex, together with Qibaoshan Cu–Au deposit, are located (Fig. 1a and b). The volcanic rocks are mainly comprised of andesitic rocks, and the intrusive complex consists of dioritic porphyries (127.4 Ma; Liu et al., unpublished data) and pyroxene monzonites (126 Ma; Zhou et al., 2003). The Qibaoshan Cu–Au deposit is principally hosted by dioritic porphyries that occur as breccia pipes, distinct from the volcanic rocks (Wang, 1991; Qiu et al., 1994). The volcanic rocks include andesite and trachyandesite and occur as massive lava flows in a graben within the Mesozoic (Jurassic–Cretaceous) continental Laiyang Basin. This basin is predominantly comprised of a suite of volcano-sedimentary rock formations. The Mesozoic strata include three volcanic rock formations; the Laiyang, the Qingshan and Wangshi Formations (SPFGSME, 2003). Andesite and trachyandesite belongs to Qingshan Formation and cover an area of ~120 km^2, with their exposures controlled by the Tanlu fault and a WE-striking fault (Fig. 1b). Moreover, many Neoproterozoic (740–760 Ma) low-grade metamorphic complexes (gneissoid granites, amphibolites and quartzite–slate–phyllite–marble association rocks) and Mesozoic granites (115–125 Ma) outcrop in the adjacent areas, in Wulian (Zhou et al., 2003, 2008; Wu et al., 2004; Huang et al., 2005, 2006; Zheng et al., 2005; Liu et al., 2008b) (Fig. 1b).

The Jiaodong adakitic volcanic rocks that are the focus of this study are trachyandesite with a microporphyritic texture. These are interlayered with andesitic breccia; no basaltic or acidic rocks are found associated with the adakitic rocks in this area. The adakitic rocks contain abundant (23–38%) phenocrysts of plagioclase and pyroxene (0.5–1.6 mm). Minor phenocrysts of amphibole and biotite are also observed. The matrix is composed of fine-grained (0.05–0.08 mm) plagioclase, magnetite, and hematite.

3. Analytical methods

Laser ablation techniques were used for zircon U–Pb age determination (Table 1). The analyses were conducted with an Elan 6100 DRC ICP-MS equipped with 193 nm excimer lasers, which is housed in the Department of Geology, Northwest University, Xi'an, China. Zircon 91500 was used as a standard and NIST 610 was used to optimize the machine. The spot diameter was 30 μm. Corrections for common-Pb were made using the method of Anderson (2002). Data were processed using the GLITTER and ISOPLOT (Ludwig, 2003) programs. Errors on individual analyses by LA-ICPMS are quoted at the 95% (1σ) confidence level. The details of the analytical procedures have been described by Yuan et al. (2004).

Whole-rock samples were trimmed to remove altered surfaces, and were cleaned with deionized water, crushed, and powdered with an agate mill. The pulverized samples were used for major, trace element, and Sr–Nd–Pb isotopic analysis. Major elements were analyzed with a PANalytical Axios-advance (Axios PW4400) X-ray fluorescence spectrometer (XRF) at the State Key Laboratory of Ore Deposit Geochemistry, Institute of Geochemistry, Chinese Academy of Sciences (IGCAS). Fused glass discs were used and the analytical precision was better than 3% (Table 2). Loss on ignition (LOI) was obtained from 1 g of powder by weighing after 1 h of calcinations at 1100 °C. Trace elements were analyzed with a POEMS ICP-MS at the National Research Center of Geoanalysis, Chinese Academy of Geosciences, following procedures described by Qi et al. (2000). The discrepancies between triplicate analyses were less than 5% for all elements.

For Rb–Sr and Sm–Nd isotope analysis, sample powders were spiked with mixed isotope tracers, dissolved in Teflon capsules

Table 1
Laser ablation ICP-MS U–Pb data of zircons in the adakitic trachyandesite (QS001) from Jiaodong, eastern NCC.

Isotopic ratios												Age(Ma)					
Spot	Th	U	Pb	Th/U	$^{238}U/^{232}Th$	$^{207}Pb/^{206}Pb$	1σ	$^{207}Pb/^{235}U$	1σ	$^{206}Pb/^{238}U$	1σ	$^{207}Pb/^{206}Pb$	1σ	$^{207}Pb/^{235}U$	1σ	$^{206}Pb/^{238}U$	1σ
1	2040	751	26.3	2.71	0.37	0.0514	0.0010	0.1385	0.0025	0.0195	0.0001	260	28	132	2	124.7	0.9
2	1387	687	20.6	2.02	0.50	0.0517	0.0012	0.1349	0.0027	0.0189	0.0001	272	33	128	2	120.9	0.9
3	2109	687	25.6	3.07	0.33	0.0668	0.0014	0.1794	0.0033	0.0195	0.0001	833	27	168	3	124.4	0.9
4	3376	812	35.0	4.16	0.24	0.0554	0.0011	0.1491	0.0025	0.0195	0.0001	429	25	141	2	124.6	0.9
5	1490	637	20.8	2.34	0.43	0.0535	0.0013	0.1412	0.0031	0.0191	0.0002	350	35	134	3	122.2	0.9
6	1071	574	17.6	1.87	0.54	0.0550	0.0012	0.1485	0.0030	0.0196	0.0002	411	31	141	3	125.1	0.9
7	3208	1013	37.3	3.17	0.32	0.0504	0.0010	0.1344	0.0024	0.0193	0.0001	213	28	128	2	123.4	0.9
8	1841	812	27.0	2.27	0.44	0.0530	0.0010	0.1472	0.0023	0.0201	0.0001	328	23	139	2	128.5	0.9
9	3552	1136	43.7	3.13	0.32	0.0606	0.0009	0.1685	0.0021	0.0202	0.0001	624	16	158	2	128.7	0.8
10	548	589	14.6	0.93	1.08	0.0540	0.0010	0.1492	0.0025	0.0200	0.0001	371	25	141	2	127.8	0.9
11	4995	1803	62.6	2.77	0.36	0.0768	0.0011	0.2002	0.0022	0.0189	0.0001	1116	12	185	2	120.6	0.8
12	1711	994	28.9	1.72	0.58	0.0570	0.0009	0.1536	0.0021	0.0195	0.0001	491	19	145	2	124.6	0.8
13	1083	1295	33.0	0.84	1.20	0.0747	0.0017	0.2073	0.0042	0.0201	0.0002	1062	28	191	4	128.0	1.0
14	3397	967	37.2	3.51	0.28	0.0539	0.0010	0.1437	0.0023	0.0193	0.0001	368	23	136	2	123.3	0.8
15	582	500	13.0	1.16	0.86	0.0536	0.0012	0.1416	0.0029	0.0192	0.0001	356	33	135	3	122.3	0.9
16	1721	978	27.4	1.76	0.57	0.0515	0.0010	0.1303	0.0023	0.0184	0.0001	262	27	124	2	117.2	0.8
17	1500	710	22.1	2.11	0.47	0.0526	0.0010	0.1395	0.0024	0.0192	0.0001	311	26	133	2	122.9	0.9
18	1382	769	22.5	1.80	0.56	0.0519	0.0011	0.1376	0.0025	0.0192	0.0001	282	28	131	2	122.7	0.9
19	831	319	11.1	2.61	0.38	0.0494	0.0013	0.1331	0.0032	0.0195	0.0002	169	41	127	3	124.6	0.9
20	995	446	15.0	2.23	0.45	0.0501	0.0011	0.1400	0.0027	0.0203	0.0002	200	32	133	2	129.4	0.9
21	1061	598	17.4	1.78	0.56	0.0514	0.0014	0.1368	0.0035	0.0193	0.0002	257	43	130	3	123.0	1.0
22	422	650	14.9	0.65	1.54	0.0566	0.0017	0.1486	0.0041	0.0191	0.0002	476	45	141	4	122.0	1.0
23	2766	1068	35.3	2.59	0.39	0.0520	0.0009	0.1366	0.0021	0.0191	0.0001	284	23	130	2	121.8	0.8
24	1849	706	24.9	2.62	0.38	0.0576	0.0009	0.1520	0.0018	0.0191	0.0001	516	16	144	2	122.2	0.8
25	550	751	20.1	0.73	1.36	0.0501	0.0008	0.1362	0.0019	0.0197	0.0001	201	20	130	2	125.9	0.8
26	1898	779	26.9	2.44	0.41	0.0489	0.0008	0.1307	0.0019	0.0194	0.0001	143	21	125	2	123.9	0.8
27	1585	971	28.2	1.63	0.61	0.0595	0.0012	0.1543	0.0027	0.0188	0.0001	586	26	146	2	120.1	0.8
28	2161	697	27.0	3.10	0.32	0.0576	0.0031	0.1568	0.0082	0.0198	0.0003	513	91	148	7	126.0	2.0

Errors are 1σ; common-Pb was corrected using the method proposed by Andersen (2002).

Table 2
Major oxides (wt.%) and trace elements (ppm) of volcanic rocks from Jiaodong, eastern North China Craton.

Sample	QS1	QS2	QS3	QS4	QS5	QS6	QS7	QS8	QS9	QS10	QS11	QS12	QS13
SiO_2	61.15	60.07	61.36	61.49	61.72	59.55	59.16	59.52	60.81	60.83	60.97	59.33	59.20
TiO_2	0.67	0.70	0.68	0.63	0.67	0.65	0.64	0.65	0.70	0.65	0.62	0.64	0.63
Al_2O_3	15.28	15.23	15.46	15.3	15.29	15.35	15.22	15.66	15.43	14.91	14.82	14.61	14.43
Fe_2O_3	6.92	6.89	6.93	6.55	6.22	6.22	6.52	6.66	6.49	6.2	6.16	6.93	6.35
MnO	0.10	0.11	0.15	0.09	0.08	0.14	0.16	0.11	0.09	0.11	0.12	0.11	0.17
MgO	2.97	3.05	3.31	3.08	3.15	3.24	3.23	2.95	3.52	2.76	2.90	3.03	3.01
CaO	2.24	3.16	1.59	1.60	2.72	4.66	5.26	4.25	3.60	4.49	4.36	5.46	5.92
Na_2O	4.89	4.83	4.51	4.70	4.51	4.37	4.58	4.56	4.79	4.28	4.19	4.39	4.27
K_2O	3.33	3.84	3.43	3.59	3.15	3.41	3.46	3.25	3.15	3.72	3.65	3.86	3.82
P_2O_5	0.40	0.41	0.40	0.37	0.40	0.38	0.35	0.38	0.41	0.37	0.36	0.37	0.36
LOI	1.87	1.36	1.78	2.02	1.59	1.62	1.37	1.35	0.54	1.17	1.32	1.21	1.95
Total	99.83	99.65	99.59	99.42	99.51	99.59	99.94	99.34	99.52	99.49	99.47	99.93	100.11
$Mg^{\#}$	46	47	49	48	50	51	50	47	52	47	48	46	48
Sc	19.9	17.9	17.6	17.6	15.6	17.4	13.9	13.5	12.6	12.9	11.7	12.6	13.6
V	108	82.2	69.0	101	181	113	78.8	67.6	134	127	101	120	77.5
Cr	101	125	274	115	90.6	104	202	140	213	93.4	107	122	166
Ni	60.4	71.0	108	60.4	113	62.3	87.1	99.0	115	61.2	68.3	85.1	103
Rb	63.7	67.8	62.7	51.8	54.7	60.2	59.9	48.6	62.5	61.8	69.3	54.7	51.1
Sr	1247	1376	1178	1124	1194	1274	1241	933	1017	989	919	1053	1291
Y	14.4	14.0	14.5	13.3	14.1	13.8	14.0	13.6	14.4	15.0	14.1	13.8	13.7
Zr	213	210	215	202	218	207	206	205	219	198	193	207	203
Nb	6.70	7.04	6.83	6.19	7.11	6.53	6.71	6.36	6.99	6.45	6.12	6.58	6.35
Ba	3516	3974	4164	3420	3347	4014	4189	3969	3248	3522	3495	3391	4263
La	73.5	67	69	58.9	74	69	70	69.4	72	71.4	62.8	65.3	69.3
Ce	140	153	153	124	151	147	137	117	156	140	127	127	133
Pr	13.0	12.8	13.0	11.6	13.0	12.8	12.1	11.2	12.9	12.1	11.1	11.1	11.5
Nd	45.6	49.9	48.1	41.3	48.0	47.7	44.6	41.8	49.5	44.9	41.5	42.0	42.7
Sm	7.72	8.50	8.06	7.14	8.27	7.98	7.70	7.11	8.21	7.64	7.14	7.48	7.11
Eu	1.78	1.97	1.85	1.60	1.84	1.85	1.85	1.53	1.85	1.86	1.49	1.68	1.53
Gd	4.98	5.57	5.20	4.53	5.17	5.49	5.41	4.75	5.39	5.35	4.61	5.09	5.25
Tb	0.73	0.76	0.74	0.66	0.71	0.74	0.71	0.66	0.73	0.71	0.67	0.69	0.66
Dy	0.60	0.62	0.62	0.55	0.57	0.60	0.58	0.54	0.59	0.57	0.55	0.55	0.55
Ho	1.56	1.57	1.59	1.40	1.46	1.54	1.48	1.43	1.53	1.49	1.40	1.46	1.41
Er	1.68	1.70	1.78	1.58	1.57	1.66	1.61	1.51	1.65	1.58	1.55	1.48	1.52
Tm	0.20	0.20	0.20	0.19	0.18	0.20	0.19	0.18	0.20	0.18	0.19	0.17	0.18
Yb	1.07	1.07	1.16	1.03	0.98	1.05	1.02	0.96	1.05	0.99	1.01	0.92	0.97
Lu	0.16	0.16	0.18	0.16	0.14	0.16	0.15	0.14	0.16	0.15	0.15	0.14	0.15
Hf	6.37	6.34	6.38	6.06	6.42	6.15	6.18	6.13	6.46	5.95	5.77	5.99	5.94
Ta	0.38	0.38	0.37	0.35	0.36	0.36	0.34	0.34	0.38	0.34	0.32	0.34	0.34
Pb	14.8	19.6	19.3	14.7	20.7	20.0	19.6	15.4	22.1	20.2	17.0	23.6	19.4
Th	20.1	20.6	20.1	18.3	19.9	19.0	18.9	17.8	20.3	19.0	18.1	18.6	18.3
U	2.37	2.18	2.31	2.55	2.86	2.73	3.30	1.57	2.77	2.72	2.27	2.61	2.11
Th/Ce	0.14	0.13	0.13	0.15	0.13	0.13	0.14	0.15	0.13	0.14	0.14	0.15	0.14
La/Yb	46.7	42.5	40.0	38.4	51.2	44.6	46.3	49.0	46.4	48.9	42.1	47.9	48.5
Sr/Y	86.6	98.3	81.2	84.3	84.8	92.7	88.4	68.8	70.5	65.9	65.4	76.3	94.2
Rb/Sr	0.05	0.05	0.05	0.05	0.05	0.05	0.05	0.05	0.06	0.06	0.08	0.05	0.04
Nb/Ta	17.9	18.8	18.4	17.8	19.6	18.1	19.6	18.9	18.5	19.0	19.1	19.2	18.7
Zr/Hf	33.4	33.2	33.7	33.3	33.9	33.6	33.4	33.5	33.9	33.3	33.5	34.6	34.2

LOI = Loss on Ignition.
$Mg^{\#} = 100 * Mg/(Mg + \sum Fe)$ atomic ratio.

with HF and HNO_3 acids, and separated by conventional cation-exchange techniques. Isotopic measurements were performed on a Finnigan MAT-262 thermal ionization mass spectrometer (TIMS) at the Isotopic Geochemistry Laboratory of Yichang Institute of Geology and Mineral Resources. Procedural blanks containing <200 pg of Sm and Nd and <500 pg of Rb and Sr were used. The mass fractionation corrections for Sr and Nd isotopic ratios were based on $^{86}Sr/^{88}Sr = 0.1194$ and $^{146}Nd/^{144}Nd = 0.7219$, respectively. Analysis of standards during the period of analysis yielded the following: NBS987 gave $^{87}Sr/^{86}Sr = 0.710246 \pm 16$ (2σ) (recommended value, 0.710245 ± 14), while La Jolla gave $^{143}Nd/^{144}Nd = 0.511863 \pm 8$ (2σ) (recommended value, 0.511859 ± 7). Lead was

Table 3
Sr–Nd–Pb isotopic compositions for the adakitic volcanic rocks from Jiaodong, eastern NCC.

Sample no.	Sm (ppm)	Nd (ppm)	$^{147}Sm/^{144}Nd$	$^{143}Nd/^{144}Nd$	$2S_m$	$(^{143}Nd/^{144}Nd)_i$	$\varepsilon_{Nd}(t)$	Rb (ppm)	Sr (ppm)	$^{87}Rb/^{86}Sr$	$^{87}Sr/^{86}Sr$	$2S_m$	$(^{87}Sr/^{86}Sr)_i$	$^{206}Pb/^{204}Pb$	$^{207}Pb/^{204}Pb$	$^{208}Pb/^{204}Pb$
QS1	8.12	57.9	0.084	0.511574	13	0.511506	−19.0	51.1	1289	0.114	0.710086	11	0.709885	17.194	15.538	38.296
QS2	8.79	61.8	0.086	0.511592	10	0.511523	−18.7	60.4	1239	0.141	0.709934	9	0.709687	17.021	15.407	37.889
QS5	9.48	66.7	0.085	0.511601	12	0.511532	−18.5	55.1	1185	0.134	0.709926	10	0.709961	17.016	15.385	37.862
QS7	9.86	69.5	0.086	0.511586	10	0.511517	−18.8	68.1	1384	0.142	0.709913	11	0.709663	16.986	15.363	37.721
QS10	8.76	63.4	0.084	0.511578	11	0.511510	−18.9	62.3	993	0.181	0.710029	10	0.709711	16.964	15.351	37.716
QS13	8.86	64.2	0.083	0.511569	9	0.511502	−19.1	61.7	1335	0.134	0.709967	10	0.709732	16.949	15.338	37.711

Chondrite uniform reservoir (CHUR) values ($^{87}Rb/^{86}Sr = 0.0847$, $^{87}Sr/^{86}Sr = 0.7045$, $^{147}Sm/^{144}Nd = 0.1967$ $^{143}Nd/^{144}Nd = 0.512638$) are used for the calculation. $\lambda_{Rb} = 1.42 \times 10^{-11}$ year^{-1} (Steiger and Jäger, 1977); $\lambda_{Sm} = 6.54 \times 10^{-12}$ year^{-1} (Lugmair and Harti, 1978).

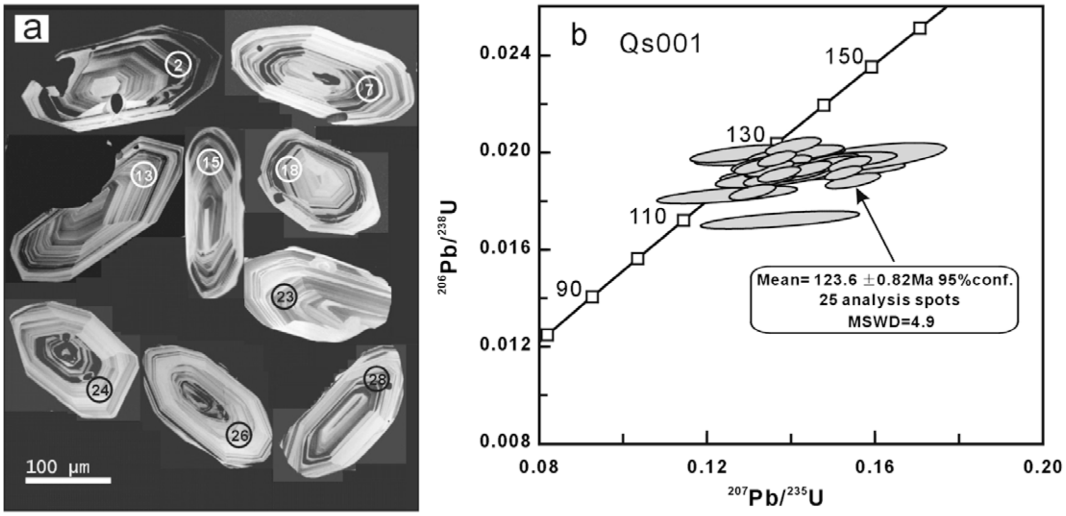

Fig. 2. Cathodoluminescence images and LA-ICPMS U–Pb Concordia diagrams for zircon from sample QS001.

separated and purified by a conventional cation-exchange technique (AG1 × 8, 200–400 resin) with diluted HBr used as the eluant. Analyses of NBS981 during the period of analysis yielded ^{204}Pb/^{206}Pb = 0.0896 ± 15, ^{207}Pb/^{206}Pb = 0.91446 ± 80 (recommended value, 0.9146 ± 3), and ^{208}Pb/^{206}Pb = 2.16171 ± 200 (Table 3).

4. Analytical results

4.1. Zircon cathodoluminescence (CL) image and U–Pb data

Zircon is abundant in the adakitic trachyandesites from Jiaodong. Zircons from trachyandesite sample QS001 were euhedral, colourless and transparent, mostly elongate-prismatic, and ranged up to 100 μm in diameter. The majority exhibited oscillatory or planar zoning in CL (Fig. 2a), a typical feature of magmatic zircon. Some grains were zoned with apparently rounded or irregular cores, mantled by euhedral overgrowths which also had oscillatory zoning (Fig. 2a). The zircons all have relatively high Th/U ratios (0.65–4.16), suggestive of a magmatic origin. On the basis of CL imagery and Th/U ratios, an igneous origin for the zircons is evident. The U–Pb zircon data are presented in Table 1. Analyses of zircon grains with oscillatory structures were concordant and yielded a weighted mean ^{206}Pb/^{238}U age of 123.6 ± 0.82 Ma ($n = 28$) (Fig. 2b). This age is interpreted as the crystallization age of the volcanic rocks.

4.2. Major and trace elements

Representative major and trace element results for the trachyandesites are listed in Table 2. On a SiO_2 vs. $K_2O + Na_2O$ diagram (Fig. 3a), all samples of the volcanic rocks fall within the field for the ‘alkaline’ rock series. Fig. 3b illustrates the K-series character of the volcanic rocks. The trachyandesites exhibit high concentrations of SiO_2 (59.16–61.72 wt.%), Sr (919–1376 ppm), and Ba (3347–4263 ppm), and relatively low levels of Al_2O_3 (14.43–15.66 wt.%), Yb (0.92–1.16 ppm), and Y (13.3–15 ppm), as well as elevated Sr/Y (65.4–98.3) and La/Yb (38.4–51.2) ratios (Fig. 4a and b). These values are similar to those typical for adakite from a subduction-environment (Defant and Drummond, 1990), except for their high K contents (K_2O = 3.15–3.86 wt.%). Furthermore, the adakitic rocks under study are characterized by high concentrations of MgO (2.9–3.52 wt.%) (Table 2; Fig. 5). Elevated values for

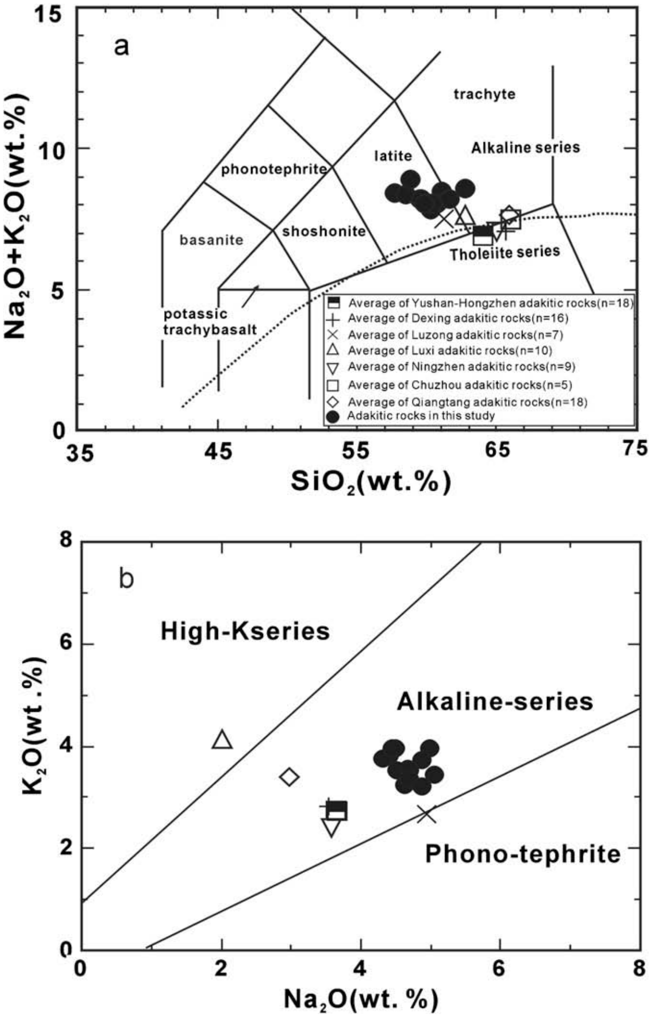

Fig. 3. (a) Chemical composition of the volcanic rocks in Jiaodong plotted in a TAS classification diagram (Le Maitre et al., 1989). Data sources for the various rock types are as follows: Qiangtang adakitic rock data are from Liu et al. (2008a), Luxi adakitic rocks from Liu et al. (2008b), Chuzhou adakitic rocks from Guo et al. (2006), Ningzhen adakitic rocks from Xu et al. (2002), Luzong adakitic rocks from Wang et al. (2006b), Dexing adakitic rocks from Wang et al. (2006a), and Yueshan-Hongzhen adakitic rocks from Wang et al. (2004); (b) K_2O vs SiO_2, series boundaries are from Middlemost (1975). The legends for the other diagrams are the same as in Fig. 3.

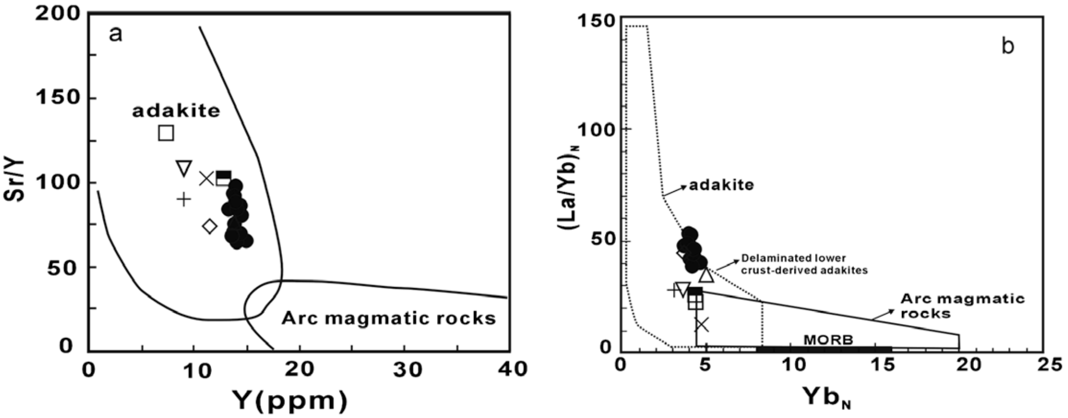

Fig. 4. Sr/Y vs. Y (a) and $(La/Yb)_N$ vs. Yb_N (b) diagrams (Defant and Drummond, 1990) of the adakitic lavas from Jiaodong, eastern NCC.

Mg# (46–52), Th (17.8–20.6 ppm), Cr (93.4–274 ppm), and Ni (60.4–115 ppm) and low Th/Ce ratios (0.13–0.15) (Table 2) are compositional features typical of adakites derived from melting of subducted oceanic crust or delaminated lower crust (Defant and Drummond, 1990; Kay et al., 1993; Drummond et al., 1996; Stern and Kilian, 1996; Sajona et al., 2000; Defant et al., 2002; Aguillón-Robles et al., 2001; Martin et al., 2005; Xu et al., 2002; Wang et al., 2004).

The Jiaodong adakitic volcanic rocks are characterized by significant enrichment in light rare earth elements (LREE), strong depletion in heavy rare earth elements (HREE), inconspicuous Eu anomalies and weakly concave middle rare earth element (MREE) patterns, as exhibited on chondrite-normalized REE diagrams (Fig. 6a). It is commonly considered that MREE patterns with clear to weak concavities imply the presence of residual amphibole in the source (Gromet and Silver, 1987). In addition, N-MORB normalized trace element patterns reveal that all samples are depleted in the high field strength elements (HFSE) Nb, Ta, and Ti, and enriched in Sr and Ba (Table 2; Fig. 6b). The REE and trace element patterns of the adakitic trachyandesites are similar to those of subducted oceanic crust-derived adakite (Defant and Drummond,1990; Kay

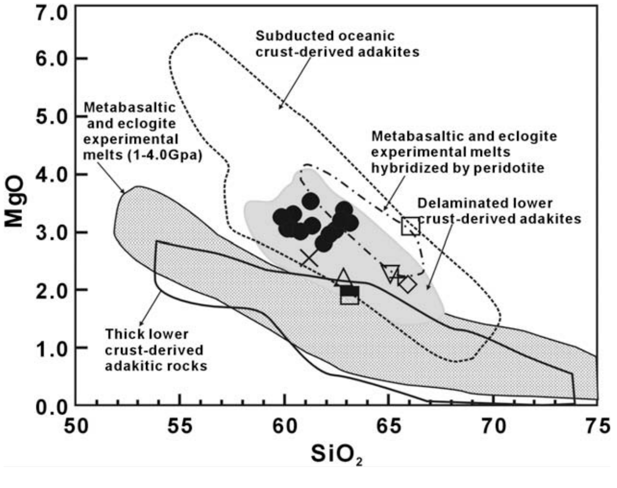

Fig. 5. MgO wt.% vs. SiO_2 (wt.%) diagrams for the Jiaodong adakitic volcanic rocks. Data for delaminated lower crust-derived adakitic rocks are from Xu et al. (2002) and Wang et al. (2004). The field of subducted oceanic crust-derived adakites is constructed using data from Defant and Drummond (1990), Kay et al. (1993), Drummond et al. (1996), Stern and Kilian (1996), Sajona et al. (2000), Aguillón-Robles et al., 2001, Defant et al. (2002) and Martin et al. (2005), and references therein. Data for thick lower crust-derived adakitic rocks are from Atherton and Petford (1993), Muir et al. (1995), Petford and Atherton (1996), Johnson et al. (1997) and Xiong et al. (2003). The field of metabasaltic and eclogite experimental melts (1–4.0 GPa) is from Rapp et al. (1991, 1999, 2002), Sen and Dunn (1994), Rapp and Watson (1995), Prouteau et al. (1999), Skjerlie and Patiño Douce (2002), and references therein. The field of metabasaltic and eclogite experimental melts hybridized with peridotite is after Rapp et al. (1999).

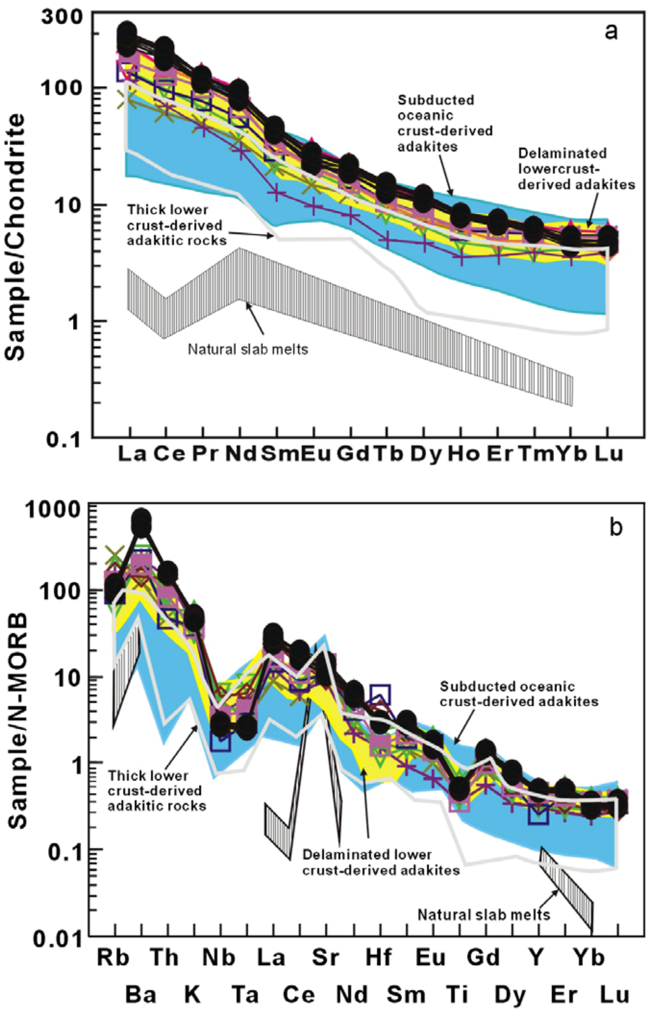

Fig. 6. Chondrite-normalized (a) and N-MORB-normalized spidergrams (b) of Jiaodong adakitic volcanic rocks from the eastern NCC. Normalized values are after Sun and McDonough (1989). The REE and trace element data for delaminated lower crust-derived adakitic rocks, subducted oceanic crust-derived adakites, and thick lower crust-derived adakites are quoted from the same data sources as those in Fig. 5. Natural slab melts are after Kepezhinskas et al. (1995).

et al., 1993; Drummond et al., 1996; Stern and Kilian, 1996; Sajona et al., 2000; Defant et al., 2002; Aguillón-Robles et al., 2001; Martin et al., 2005; Fig. 6a) and/or delaminated lower crust-derived adakitic rocks (e.g., Kay and Kay, 1993; Defant et al., 2002; Xu et al., 2002; Wang et al., 2004, 2006a,b; Guo et al., 2006; Liu et al., 2008a,c), but unlike those of adakitic rocks directly derived from partial melting of a thickened crust (Atherton and Petford, 1993; Muir et al., 1995; Petford and Atherton, 1996; Johnson et al., 1997; Xiong et al., 2003) or natural slab melt (Kepezhinskas et al., 1995) (Fig. 6a and b).

4.3. Sr–Nd–Pb isotopic ratios

Isotopic data for Sr, Nd and Pb were obtained from representative Jiaodong trachyandesite samples (Table 3). These adakitic rocks display very uniform initial $^{87}Sr/^{86}Sr$ ratios ranging from 0.7097 to 0.7099, and relatively small variation in initial. $\varepsilon_{Nd}(t)$ values (−18.5 to −19.1); which distinguish from the adikitic rocks produced by partial melting of subducted MORB with low Sr isotopic ratios and positive $\varepsilon_{Nd}(t)$ (e.g., on Cook Island, Stern and Kilian, 1996; and at Cerro Pampa, Kay et al., 1993). The Jiaodong adakitic trachyandesite, together with the Sulu adakitic rocks (Guo et al., 2006), fall within the range of the isotopic composition of the late Mesozoic intermediate-acidic rocks from the Sulu belt (Zhao et al., 1997; Zhou and Lu, 2000; Fan et al., 2001; Guo et al., 2004; Huang et al., 2005; Yang et al., 2005) (Fig. 7). However, the Sr–Nd isotopic compositions differ from those of subducted oceanic crust-derived adakites (Defant et al., 1992; Kay et al., 1993; Sajona et al., 2000; Aguillón-Robles et al., 2001), thick lower crust-derived adakites (Muir et al., 1995; Petford and Atherton, 1996), other delaminated lower crust-derived adakitic volcanic rocks (Xu et al., 2002; Wang et al., 2006a,b; Liu et al., 2008a,b), and the Jurassic–Cretaceous intermediate-acidic rocks in the eastern SCB (Wang, 2000; Xu et al., 2002; Wang et al., 2003a,b) (Fig. 7).

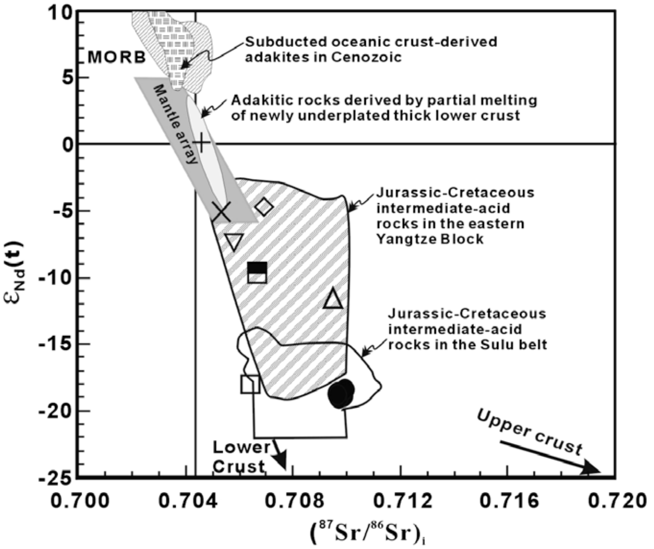

Fig. 7. Nd–Sr isotopic compositions of the adakitic lavas. The data for adakitic rocks directly derived from a thick crust are after Atherton and Petford (1993), Muir et al. (1995) and Petford and Atherton (1996); those for Cenozoic subducted oceanic crust-derived adakites are after Defant et al. (1992), Kay et al. (1993) and Sajona et al. (2000) and Aguillón-Robles et al. (2001). The values for Jurassic–Cretaceous intermediate–acid rocks in the eastern Yangtze Block are from Wang (2000) and Xu et al. (2002), and Wang et al. (2003a,b); those for MORB are from Mahoney et al. (1998), Xu et al. (2003), Tribuzio et al. (2004) and Xu and Castillo (2004). The late Mesozoic intermediate-acidic rock data from the Sulu belt are from Zhao et al. (1997), Zhou and Lu (2000), Fan et al. (2001), Guo et al. (2004), Huang et al. (2005) and Yang et al. (2005).

Lead isotopic ratios in Jiaodong adakitic trachyandesites are characterized by $^{206}Pb/^{204}Pb = 16.949–17.194$, $^{207}Pb/^{204}Pb = 15.338–15.538$, $^{208}Pb/^{204}Pb = 37.711–38.296$ (Table 3). These compositional characteristics are comparable to those of Mesozoic igneous rocks from the NCC and Dabie orogen (Zhang et al., 2006; Liu et al., 2004, 2006; Yang et al., 2004, 2005; Huang et al., 2005, 2006; Zhao et al., 2007; Liu et al., 2008b,d), having a clear affinity to EM1 (Xie et al., 2006); however, they differ from those of the Mesozoic igneous rocks from the SCB (EM2-like) (Yan et al., 2003) and/or MORB from the Pacific or Central Indian oceans (Mahoney et al., 1989; White et al., 1987) (Fig. 8).

5. Discussion

5.1. Petrogenesis

5.1.1. Origin of the adakitic magmas

Our studies of major- and trace-elements indicates that the Jiaodong adakitic rocks are geochemically similar to those of adakites formed from melting of subducted oceanic crust or delaminated lower crust (Table 2; Fig. 6a and b). Nevertheless, the various possibilities for generating adakitic rocks at Jiaodong should be discussed. Tectonic reconstructions do not favour a subduction-zone scenario in eastern China during the Early Cretaceous (e.g., Lu et al., 1997; Li, 2000; Xu et al., 2002). In addition, although the Jiaodong adakites have EM1-like features, which may suggest an origin of the subduction of ancient oceanic crust plus a minor proportion of sediment (Rehkämper and Hofmann, 1997; Stracke et al. 2003). Furthermore, subduction of a remnant ocean (the Sulu Sea) may have occurred during the Late Jurassic and Early Cretaceous (Wu et al., 2002, 2003). The adakitic trachyandesites, however, have low $^{206}Pb/^{204}Pb$ ratios, which indicate that their source is neither subducted oceanic slab nor sediment. Moreover, if these adakitic magmas were formed by partial melting of a subducted oceanic crust or sedimentary material, they would be expected to have MORB-like Sr–Nd isotopic compositions ($\varepsilon_{Nd}(t) > 6$, Sulu Sea, Xu and Castillo, 2004) and high $^{206}Pb/^{204}Pb$ ratios (>18) (e.g., Sulu Sea, Xu and Castillo, 2004; oceanic sediments in the west Pacific, Castillo et al., 1994; Shimoda et al., 1998), but this is not the case.

An alternative mechanism of generating adakitic magma is through assimilation–fractional crystallization (AFC) processes, involving basaltic magma. This has been proposed for the origin of adakites from Camiguin Island in the Philippines (Castillo et al., 1999). Similar processes, however, seem unlikely to have produced the Jiaodong adakitic magmas, as coexisting mafic rocks, with the exception of only a few mafic dykes, are lacking from the volcanic sequence (SBGMR, 1995); fractionation of such small volumes of mafic dykes would not result in the large volumes of the adakitic volcanic rocks observed. In addition, in plots of La/Yb vs. La and Ni vs. Th (Fig. 9a and b), the data are more consistent with a partial melting trend rather than a trend for fractional crystallization, suggesting that the former is the dominant mechanism in controlling the compositional variability within the Jiaodong adakitic volcanic rocks. However, the investigated adakites likely experienced some fractional crystallization as abundant plagioclase + pyroxene are observed in the rocks. Otherwise, no correlations exist between SiO_2 and $\varepsilon_{Nd}(t)$ or $(^{87}Sr/^{86}Sr)$ as shown in Fig. 9c and d, clearly indicating that they were probably not generated from an assimilation and fractional crystallization (AFC) – like process. If crustal contamination was extensive, correlations between SiO_2 and Sr and Nd isotopic compositions would be expected (Castillo et al., 1999). Likewise, the Jiaodong adakitic volcanic rocks cannot have been produced by direct melting of mantle peridotite, as these scenarios would not produce melts more silicic than andesite or boninite (~55 wt.% SiO_2) (Green, 1980; Jahn and Zhang,

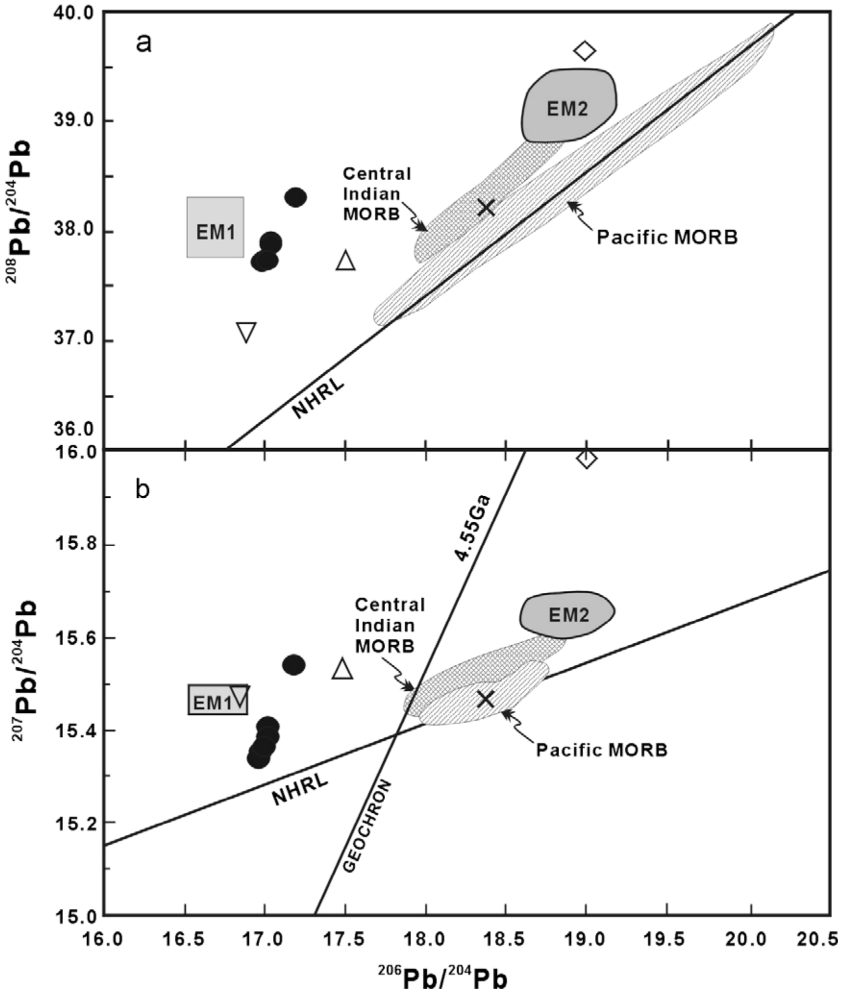

Fig. 8. $^{208}Pb/^{204}Pb$ and $^{207}Pb/^{204}Pb$ vs. $^{206}Pb/^{204}Pb$ diagrams for the adakitic rocks from Jiaodong, eastern NCC. The fields for Indian MORB and Pacific MORB, OIB, NHRL and 4.55 Ga geochron are after Zou et al. (2000) and Hart (1984), respectively.

1984; Baker et al. 1995), which is contrary to observation (59–62 wt.% SiO_2).

Based on the above interpretations, melting of mafic lower crust material is thought to be the most likely scenario for the origin of the Jiaodong adakitic rocks discussed herein. It is generally believed that basaltic melt underplating can result in melting of mafic lower crust and production of adakitic rocks (Atherton and Petford, 1993). If adakitic magmas were derived directly from partial melting of mafic lower crust, they should have relatively low MgO, Cr, and Ni contents (Kay, 1978; Rapp et al., 1999). However, the Jiaodong adakitic rocks show relatively high concentrations of these species (Table 2; Fig. 5), as well as high $Mg^{\#}$ values (Table 2). This may suggest that the primary adakitic melts have interacted to some extent with peridotitic mantle material (Kay, 1978; Rapp et al., 1999). Hence, we propose that the investigated Jiaodong adakitic trachyandesites formed by melting of delaminated lower crust within the lithospheric mantle. Furthermore, as the pristine adakitic melts ascended, they reacted with peridotite to produce the observed elevated MgO, Cr, Ni contents and $Mg^{\#}$ values that typify these samples.

Because the Wulian region is located close to the suture zone (Wulian-Yantai fault) between the NCC and SCB, it is necessary to assess the influence, if any of the Mesozoic lithotectonic units present within the Wulian region. While Mesozoic mantle-derived mafic rocks are scarce, granites are widespread in the Wulian region (115–125 Ma) (Zhou et al., 2003; Huang et al., 2005, 2006; Liu et al., 2008b). The geochemical characteristics of these granites suggest that their sources mainly derived from the NCC, and that the granites resulted from melting of metasomatized NCC mantle with subsequent crystal fractionation (Liu et al., 2008b). Furthermore, the Pb isotopic compositions (Table 3; Fig. 8) of the Wulian adakitic magmas (EM1-like features) indicate that these rocks were derived from the NCC rather than SCB. Accordingly, the shallow (crust) and deep (mantle) levels in the Wulian region both belong to the NCC. The Jiaodong adakitic rocks are characterized by high La/Yb and Sr/Y ratios and low Y and Yb contents (Table 2; Fig. 4a and b), indicating the residual presence of garnet and the absence of plagioclase in the source (Defant and Drummond, 1990; Atherton and Petford, 1993; Rapp and Watson, 1995; Drummond et al., 1996; Defant and Kapezhinskas, 2001; Rapp et al., 1999, 2003; Castillo, 2006). Insignificant plagioclase fractionation is further supported by weak correlations between SiO_2 vs. Al_2O_3 and Sr (not shown) and an absence of negative Sr anomalies in the primitive mantle-normalized trace elements patterns for the adakites (Fig. 6b); as both Sr ($D^{plagioclase/melt} = 3.4$) (Bacon and Druitt, 1988) and Al ($D^{plagioclase/melt} > 1.2$) (Icenhower and London, 1996) are compatible in plagioclase, crystal fractionation of plagioclase can result in negative correlations between SiO_2 vs. Al_2O_3 and Sr, as well as a negative Sr anomaly. Because such a source is generally thought to occur at depths of >40 km (>1.2 GPa) (Rapp and Watson, 1995; Petford and Atherton, 1996), the crustal thickness in the study area had to have been at least 40 km when the adakitic

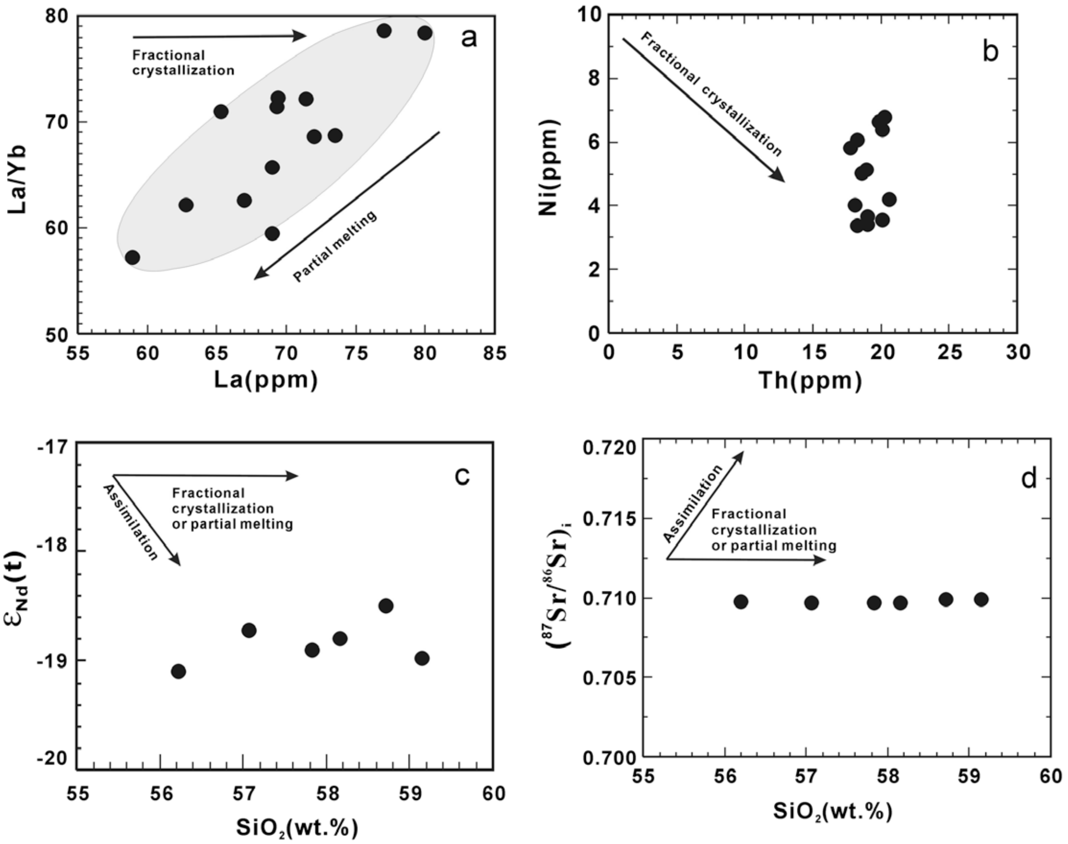

Fig. 9. Plots of La/Yb vs. La (a), ε_{Nd}(t) values vs. SiO_2 (b), and initial $^{87}Sr/^{86}Sr$ ratios vs. SiO_2 (c) for the adakitic volcanic rocks in Jiaodong, eastern NCC.

magmas were produced in the Early Cretaceous. Generally, Nb partitions strongly into amphibole under equilibrium conditions (Pearce and Norry, 1979), whereas Ti partitions into rutile under hydrous mantle conditions (Tatsumi, 1986). Both elements are strongly depleted in the Jiaodong adakitic rocks, which suggesting that amphibole and rutile were stable within the source residues when the adakitic magmas were segregated. As noted above, the source of the adakitic rocks was most probably amphibole-bearing or rutile-bearing eclogitic lower crust. If the source has contained residual amphibole, magma directly derived from this source should have relatively higher Rb/Sr ratio than Primitive Mantle (~0.03) (Ionov et al., 1997). As amphibole commonly has Rb/Sr ratios lower than or close to that of Primitive Mantle (PM), its absence can yield whole-rock Rb/Sr ratios higher than the PM value (~0.03). Relatively higher Rb/Sr ratios (0.04–0.08) for the adakitic rocks (Table 2) thus accept this possibility. The amphibole residue

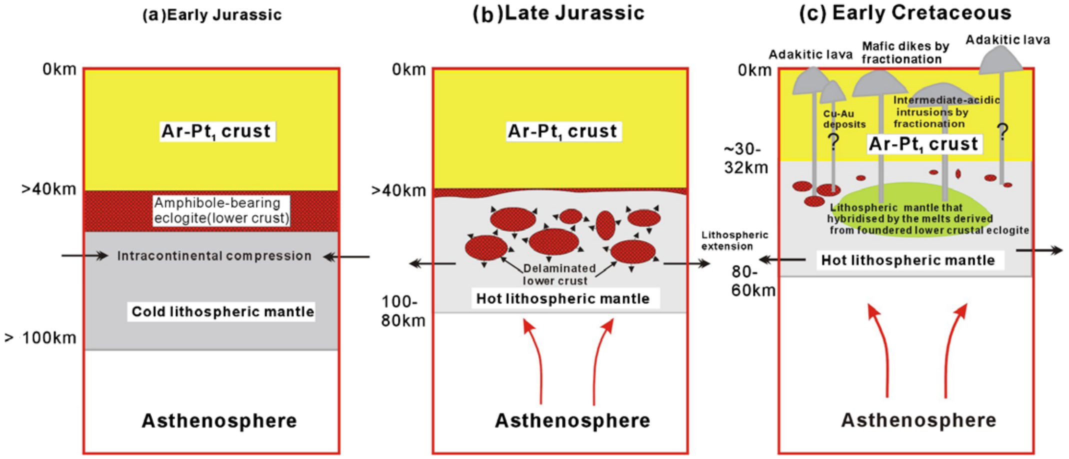

Fig. 10. Suggested model to produce Jiaodong adakitic lava via foundering of lower crust in the Early Cretaceous. (a) Relatively thick crust due to intercontinental compression at 205–185 Ma (Li, 1994). The thick lower crust was composed of amphibole-bearing eclogite. (b) The thick eclogitic lower crust was removed through delamination or foundering through density instability and fell into the underlying hot lithospheric mantle at 185–165 Ma (Li et al., 2002). At the same time, the silicic melts that originated from the melting of silica-saturated eclogites would have reacted extensively with the overlying mantle peridotite to produce olivine-free pyroxenite. (c) Lithospheric foundering which resulted in lithospheric extension and asthenospheric upwelling. Decompressional melting of the hybridized lithospheric mantle and residual ecologic lower crust would have produced pristine basaltic and adakitic melts; subsequently, intermediate-acidic intrusions and mafic dykes were formed by the fractionation of basaltic magma, and the adakitic rocks in this study were generated by reaction of pristine adakitic melts with the surrounding mantle peridotite.

within the source is also indicated by the enriched MREE pattern of the adakitic rocks (Fig. 6a). In contrast, If the source is inferred to have contained rutile residue, the adakitic rocks would be characterized by elevated super-chondritic Nb/Ta ratios (chondritic ratio: 19.9 ± 0.6) and Zr/Hf ratios (chondritic ratio: 34.3 ± 0.3) with strongly decreasing Nb and Ta concentrations (Münker et al., 2003; Xiong et al., 2005; Liu Y S et al., 2008). Indeed, the adakitic rocks in this study are characterized by relatively lower Nb/Ta ratios (17.8–19.6) and Zr/Hf ratios (33.2–34.6) compared to chondrite (Table 2). Therefore, we suggest a amphibole-bearing eclogitic lower crust source for the adakitic rocks (Fig. 10a and b).

5.1.2. Genetic process of the adakitic magmas

Based on the above discussion, we propose a model in which lower crustal delamination of the NCC coincided with adakitic magmatism (Fig. 10). Subduction in the Triassic (~240–220 Ma) of a continental slab during the collision between the NCC and the SCB formed a thickened crust at the plate margin (e.g., Li et al., 1993; Zheng et al., 2002). The resulting intracontinental compression (~205–185 Ma) between the two blocks further thickened the crust and the increase in pressure and temperature might have converted mafic rocks in the lower crust into amphibole-bearing eclogites (Li, 1994). Eclogite formed by high to ultrahigh pressure metamorphism of basaltic rock, achieving a density exceeding that of lithospheric mantle peridotite by some 0.2–0.4 g cm^{-3} (Rudnick and Fountain, 1995). The high density of such garnet-bearing mafic rocks in the lower crust leads to delamination (Kay and Kay, 1991, 1993; Rudnick, 1995; Ducea and Saleeby, 1998; Xu et al., 2002; Wang et al., 2004) or foundering (Arndt and Goldstein, 1989; Ducea and Saleeby, 1998; Gao et al., 2004; Zandt et al., 2004). Li et al. (2002) have suggested foundering of eclogitic lower crust in the Dabie-Sulu belts during the period 185–165 Ma. Likewise, we infer that source materials in the lower parts of the thickened crust (>40 km) in the study area consisted of amphibole-bearing eclogitic material that sank into the lithospheric mantle (Fig. 10a and b). Eclogites have lower melting temperatures than mantle peridotites (Yaxley and Green, 1998; Yaxley, 2000; Rapp et al., 1999; Kogiso et al., 2003; Sobolev et al., 2005, 2007). Consequently, most silica-saturated eclogites would be heated by the heat flux from the upwelling asthenosphere during foundering, inducing dehydration melting and the generation of silicic melts (tonalite to trondhjemite). These materials may hybridize variably with overlying mantle peridotite to produce an olivine-free pyroxenite, which, if subsequently melted, can generate basaltic melt (Kogiso et al., 2003; Sobolev et al., 2005, 2007; Herzberg et al., 2007; Gao et al., 2008). During the late Mesozoic (Early Cretaceous), further episode of lithospheric (lower crust or mantle) foundering occurred beneath the study area, similar to that appeared in the Dabie-Sulu belt during the period 130–110 Ma (Li et al., 2002). This event triggered asthenospheric upwelling, sudden uplift of the Earth's surface, and lithospheric extension and thinning. Decompressional melting of the olivine-free pyroxenite produced basaltic melts; magma fractionation subsequently formed large volumes of Mesozoic intermediate-acidic intrusions and mafic dykes in the Jiaodong and Sulu-Dabie belts (Zhang et al., 2006; Liu et al., 2004, 2006; Yang et al., 2004, 2005; Huang et al., 2005, 2006; Zhao et al., 2007; Liu et al., 2008b) (Fig. 10c), where the mafic intrusions are observed to be scarce. Furthermore, the residual amphibole-bearing eclogitic lower crust was heated within the lithospheric mantle producing the pristine adakitic melts. These adakitic melts ascended and interacted with mantle peridotite to form the Jiaodong adakitic volcanic rocks with their relatively high MgO, Cr, and Ni contents (Fig. 5 and Table 2). As indicated by the negative Fe/Mn–Yb correlations and positive correlation between Sc and Yb (Fig. 11a and b). Because the primary adakitic melts mixed by mantle peridotite will be clinopyroxene-and garnet-enriched, this can account for the observed correlations in Yb vs. Fe/Mn–Yb ratio and Sc (Liu et al., 2008).

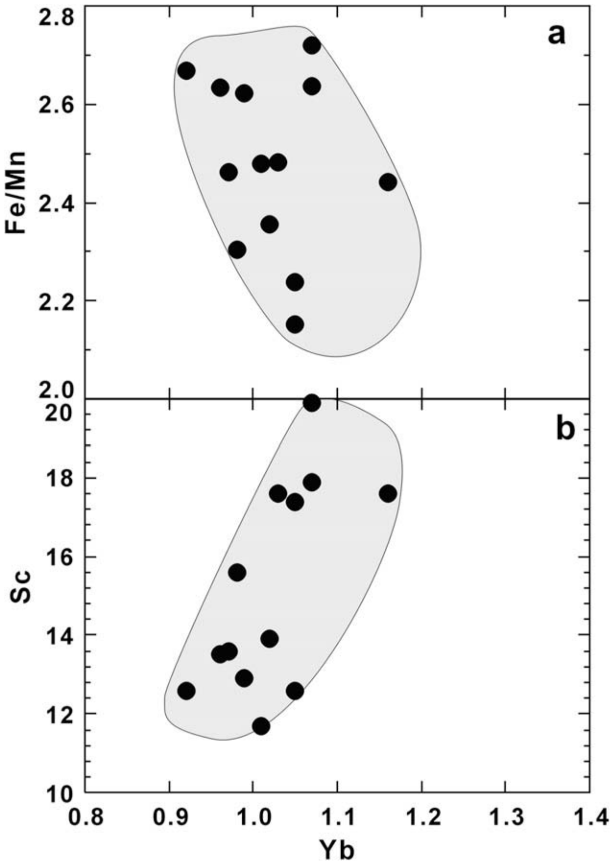

Fig. 11. Plots of Yb vs. Fe/Mn ratio and Sc for the adakitic rocks.

5.2. Tectonic implications

It is generally accepted that at least 100 km of Archaean to Proterozoic lithospheric mantle was removed from beneath large areas of east China during the late Mesozoic to the Cenozoic eras (Tertiary) (Menzies et al., 1993a,b; Griffin et al., 1998; Xu et al., 2000; Xu, 2001; Gao et al., 2002; Wu et al., 2003; Wilde et al., 2003; Zhang et al., 2004). The exact timing and mechanism of lithospheric thinning, however, remains controversial. Based on previous studies, Wu et al. (2003) proposed that in the late Mesozoic, between 130 and 120 Ma, lithospheric removal beneath eastern China was at its greatest. Theoretically, lithospheric foundering would result in lithospheric thinning, coeval magmatism (Kay and Kay, 1993), and the giant gold deposits of the eastern NCC (Yang and Zhou, 2001). Late Mesozoic magmatic activities and the formation of the giant gold deposits in Jiaodong mostly occurred between 130 and 110 Ma (Liu et al., 2001; Zhai et al., 2001; Yang et al., 2006); we thus suggest that 130–110 Ma was a dominant period for the lithospheric removal beneath Jiaodong in the eastern NCC.

Alternatively, the destruction of the NCC Archaean keel can been explained by two additional mechanisms, i.e., thermo-chemical erosion of the Archaean lithospheric mantle by upwelling asthenosphere (Menzies et al., 1993a,b, 2007; Griffin et al., 1998) and transformation of lithospheric to asthenospheric mantle by addition of melts (Zhang et al., 2007), or melts and water from a subducting slab (Niu, 2005). None of these processes, however, can explain the production of adakitic magmas from foundered lower crust, as is observed in the compositions of adakitic rocks from the study area in Jiaodong. We therefore suggest that lithospheric thinning underneath Jiaodong was caused by the removal of the lower lithosphere (mantle and lower crust). According to the source discussions, the crustal thickness in the study area was at least 40 km when the adakitic magmas were produced at 123.6 ± 0.82 Ma. However, the present crustal thickness in the Jiaodong area is only 30–32 km, according to calculations based on gravity and magnetism by Shi et al. (1989) and Jiang et al. (2000) and geophysical survey data of Xu and Zhao (2004). These data imply that the Mesozoic continental crust in the study area was thicker (>40 km) than the present crust, and that the Jiaodong lower crust therefore has most likely undergone an intense process of thinning.

6. Conclusions

Based on the geochronological, geochemical, and Sr–Nd–Pb isotopic studies reported in this study, we draw the following conclusions:

(1) The volcanic rocks from Jiaodong, located in the eastern NCC, have an adakitic geochemical affinity. Zircon U–Pb dating of this adakitic trachyandesite yields an eruption age of 123.6 ± 0.82 Ma.
(2) These adakitic rocks were derived from the melting of delaminated rutile-bearing ecologitic lower crust, triggered by heat flux from the upwelling asthenosphere, with residual garnet and amphibole in their source. In addition, these adakitic rocks are characterized by relatively high MgO, Cr, and Ni contents and high $Mg^{\#}$ values, all of which indicate that pristine magmas reacted with mantle peridotite during ascent.
(3) It is proposed that intense lithospheric thinning beneath Jiaodong of eastern China occurred between 110 and 130 Ma due to the foundering of the lower lithosphere (mantle and lower crust).

Acknowledgements

The authors would like to thank Professor Bor-Ming Jahn and Jun-Tang and three anonymous reviewers for their constructive reviews of this manuscript. I also thank Dr. L. Jennifer for quickly handling the manuscript. This research was supported by the Knowledge Innovation Project (KZCX2-YW-111-03), the National Nature Science Foundation of China (Nos. 40673029, 40773020, 40634020, 90714010 and 40521001) and Chinese Ministry of Education (No. B07039). We are grateful to Gui-xiang Yu for help with the analysis of Sr, Nd, and Pb isotopes. Dr. Xiao-ming Liu, Hong-Lin Yuan and Shao-cong Lai are thanked for help with Zircon U–Pb dating. Thanks are also due to Wei-qing Sun for providing some regional geological data. Pacific Edit reviewed the manuscript prior to submission.

References

Aguillón-Robles, A., Caimus, T., Bellon, H., Maury, R.C., Cotton, J., Bourgois, J., Michaud, F., 2001. Late Miocene adakites and Nb-enriched basalts from Vizcaino Peninsula, Mexico: indicators of East Pacific Rise subduction below southern Baja California. Geology 29, 531–534.

Andersen, T., 2002. Correction of common lead in U–Pb analyses that do not report ^{204}Pb. Chemical Geology 192, 59–79.

Arculus, R.J., Lapierrre, H., Jaillard, E., 1999. Geochemical window into subduction and accretion processes: raspas metamorphic complex, Ecuador. Geology 27, 547–550.

Arndt, N.T., Goldstein, S.L., 1989. An open boundary between lower continental crust and mantle: its role in crust. Tectonophysics 161, 201–212.

Atherton, M.P., Petford, N., 1993. Generation of sodium-rich magmas from newly underplated basaltic crust. Nature 362, 144–146.

Bacon, C.R., Druitt, T.H., 1988. Compositional Evolution of the Zoned Calcalkaline Magma Chamber of Mount-Mazama, Crater Lake, Oregon. Contributions to Mineralogy and Petrology 98 (2), 224–256.

Baker, M.B., Hischmann, M.M., Ghiorso, M.S., Stolper, E.M., 1995. Compositions of near-solidus peridotite melt from experiments and thermodynamic calculations. Nature 375, 308–311.

Castillo, P.R., 2006. An overview of adakite petrogenesis. Chinese Science Bulletin 51, 257–268.

Castillo, P.R., Janney, P.E., Solidum, R.U., 1999. Petrology and geochemistry of Camiguin Island, southern Philippines: insights to the source of adakites and other lavas in a complex arc setting. Contributions to Mineralogy and Petrology 134, 33–51.

Castillo, P.R., Pringle, M.S., Carlson, R.W., 1994. East Mariana basin tholeiites: cretaceous intraplate basalts or rift basalts related to the Ontong Java plume? Earth and Planetary Science Letters 123, 139–154.

Chung, S.L., Liu, D.Y., Ji, J.Q., Chu, M.F., Lee, H.Y., Wen, D.J., Lo, C.H., Lee, T.Y., Qian, Q., Zhang, Q., 2003. Adakites from continentla collision zones: melting of thickened lower crust beneath southern Tibet. Geology 31, 1021–1024.

Defant, M.J., Jackson, T.E., Drummond, M.S., De Boer, J.Z., Bellon, H., Feigenson, M.D., et al., 1992. The geochemistry of young volcanism throughout western Panama and southeastern Costa Rica: an overview. Journal of the Geological Society, London 149, 569–579.

Defant, M.J., Drummond, M.S., 1990. Derivation of some modern arc magmas by melting of young subducted lithosphere. Nature 347, 662–665.

Defant, M.J., Kepezhinskas, P., 2001. Evidence suggests slab melting in arc magmas: eos 82, 65–69. (Transactions, American Geophysical Union).

Defant, M.J., Kepezhinskas, P., Defant, M.J., Xu, J.F., Kepezhinskas, P., Wang, Q., Zhang, Q., Xiao, L., 2002. Adakites: some variations on a theme. Acta Petrologica Sinica 18, 129–142.

Drummond, M.S., Defant, M.J., Kepezhinskas, P.K., 1996. Petrogenesis of slab-derived trondhjemite-tonalite-dacite/adakite magmas. Trans: Royal Society Edinburg Earth Science 87, 205–215.

Ducea, M., Saleeby, J., 1998. Crustal recycling beneath continental arcs: silica-rich glass inclusions in ultramafic xenoliths from the Sierra Nevada, California. Earth and Planetary Science Letters 156, 101–116.

Fan, W.M., Guo, F., Wang, Y.J., Lin, G., Zhang, M., 2001. Postorogenic bimodal volcanism along the Sulu orogenic belt in eastern China. Physics and Chemistry of the Earth Science 26, 733–746.

Gao, S., Rudnick, R.L., Carlson, R.W., McDonough, W.F., Liu, Y.S., 2002. Re–Os evidence for replacement of ancient mantle lithosphere beneath the North China craton. Earth Planetary Science Letters 198, 307–322.

Gao, S., Rudnick, R.L., Xu, W.L., Yuan, H.L., Liu, Y.S., Walker, R.J., Puchtel, I., Liu, X.M., Huang, H., Wang, X.R., Yang, J., 2008. Recycling deep cratonic lithosphere and generation of intraplate magmatism in the North China Craton. Earth and Planetary Science Letters 270, 41–53.

Gao, S., Rudnick, R., Yuan, H.L., Liu, X.M., Liu, Y.S., Xu, W.L., Ling, W.L., Ayers, J., Wang, X.C., Wang, Q.H., 2004. Recycling lower continental crust in the north China craton. Nature 432, 892–897.

Green, T.H., 1980. Island-arc and continent-building magmatism: a review of petrogenetic models based on experimental petrology and geochemistry. Tectonophysics 63, 367–385.

Griffin, W.L., Zhang, A., O'Reilly, S.Y., Ryan, C.G., 1998. Phanerozoic evolution of the lithosphere beneath the Sino-Korean Craton. In: Flower, M., Chung, S.L., Lo, C.H., Lee, T.Y. (Eds.), Mantle Dynamics and Plate Interactions in East Asia, Geodynamics Volume, vol. 27. American Geophysical Union, pp. 107–126.

Gromet, L.P., Silver, L., 1987. REE variations across the Peninsular Ranges Batholith: implications for batholithic petrogenesis and crustal growth in magmatic arcs. Journal of Petrology 28, 75–125.

Guo, F., Fan, W.M., Li, C.W., 2006. Geochemistry of late Mesozoic adakites from the Sulu belt, eastern China: magma genesis and implications for crustal recycling beneath continental collisional orogens. Geological Magazine 143, 1–13.

Guo, F., Fan, W.M., Wang, Y.J., Zhang, M., 2004. Origin of early Cretaceous calc-alkaline lamprophyres from the Sulu orogen in eastern China: implications for enrichment processes beneath continental collisional belt. Lithos 78, 291–305.

Hart, S.R., 1984. A large-scale isotope anomaly in the Southern Hemisphere mantle. Nature 309, 753–757.

Herzberg, C., Asimow, P.D., Arndt, N., Niu, Y., Lesher, C.M., Fitton, J.G., Cheadle, M.J., Saunders, A.D., 2007. Temperatures in ambient mantle and plumes: constraints from basalts, picrites, and komatiites. Geochemisty, Geophysics, and Geosystems 8, Q02006. doi:10.1029/2006GC001390.

Hou, Z.Q., Gao, Y.F., Qu, M., Rui, Z.Y., Mao, X.X., 2004. Origin of adakitic intrusives generated during mid-Miocene east-west extension in southern Tibet. Earth and Planetary Science Letters 220, 139–155.

Huang, J., Zheng, Y.F., Wu, Y.B., Zhao, Z.F., 2005. Geochemistry of elements and isotopes in igneous rocks from the Wulian region in the Sulu orogen. Acta Petrologica Sinica 21, 545–568.

Huang, J., Zheng, Y.F., Zhao, Z.F., Wu, Y.B., Zhou, J.B., Liu, X.M., 2006. Melting of subducted continent: element and isotopic evidence for a genetic relationship between Neoproterozoic and Mesozoic granitoids in the Sulu orogen. Chemical Geology 229, 227–256.

Icenhower, J.P., London, D., 1996. Experimental partitioning of Rb, Cs, Sr, and Ba between alkali feldspar and peraluminous melt. American Mineralogist 81, 719–734.

Ionov, D.A., O'Reilly, S.Y., Griffin, W.L., 1997. Volatile-bearing minerals and lithophile trace elements in the upper mantle. Chemical Geology 141, 153–184.

Jahn, B.M., Zhang, J.Q., 1984. Archean granulite gneisses from eastern Sino-Korean Province, China: rare earth geochemistry and tectonic implication. Contributions to Mineralogy and Petrology 85, 224–243.

Jiang, W.W., Hao, T.Y., Jiao, C.M., Song, H.B., 2000. The characters of gravity and magnetic fields and crustal structure from Qingzhou to Muping, Shandong Province. Geophysics Processes 15 (4), 18–26.

Johnson, K., Barnes, C.G., Miller, C.A., 1997. Petrology, geochemistry, and genesis of high-Al tonalite and trondhjemites of the Cornucopia stock, Blue Mountains, Northeastern Oregon. Journal of Petrology 38, 1585–1611.

Jull, M., Kelemen, P.B., 2001. On the conditions for lower crustal convective instability. Journal of Geophysical Research 106, 6423–6446.

Kay, R.W., Kay, S.M., 2002. Andean adakites: three ways to make them. Acta Petrology Sinica 18, 303–311.

Kay, R.W., Kay, S.M., 1991. Creation and destruction of lower continental crust. International Journal of Earth Sciences (Geol. Rundsch) 80, 259–278.

Kay, R.W., Kay, S.M., 1993. Delamination and delamination magmatism. Tectonophysics 219, 177–189.

Kay, R.W., 1978. Aleutian magnesian and esites–melts from subducted Pacific Ocean crust. Journal of Volcanology and Geothermal Research 4, 117–132.

Kay, S.M., Ramos, V.A., Marquez, M., 1993. Evidence in Cerro Pampa volcanic rocks of slab melting prior to ridge trench collision in southern South America. Journal of Geology 101, 703–714.

Kepezhinskas, P.K., Defant, M.J., Drummond, M., 1995. Na metasomatism in the island-arc mantle by slab melt–peridotite interaction: evidence from mantle interaction-evidence from mantle xenoliths in the north Kamchatka arc. Journal of Petrology 36, 1505–1527.

Kogiso, T., Hirschmann, M.M., Frost, D.J., 2003. High-pressure partial melting of garnet pyroxenite: possible mafic lithologies in the source of ocean island basalts. Earth and Planetary Science Letters 216, 603–617.

Lai, S.C., Qin, J.F., Li, Y.F., 2007. Partial melting of thickened Tibetean Crust: geochemical evidence from Cenozoic adakitic volcanic rocks. International Geological Review 49, 357–373.

Le Maitre, R.W., Bateman, P., Dudek, Keller, A.J., Lameyre Le Bas, M.J., Sabine, P.A., Schmid, R., Sorensen, H., Streckeisen, A., Wolley, A.R., Zanetti, B., 1989. A Classification of Igneous Rocks and Glossary of Terms. Blackwell, Oxford. pp. 193.

Li, S.G., Xiao, Y.L., Liou, D.L., Chen, Y.Z., Ge, N.J., Zhang, Z.Q., Sun, S.S., Cong, B.L., Zhang, R.Y., Hart, S.R., Wang, S.S., 1993. Collision of the North China and Yangtze blocks and formation of coesite-bearing eclogites: timing and process. Chemical Geology 109, 89–111.

Li, S.G., Huang, F., Li, H., 2002. Post-collisional delamination of the lithosphere beneath Dabie-Sulu orogenic belt. Chinese Science Bulletin 46, 1487–1490.

Li, Z.X., 1994. Collision between the North and South China Blocks: a crustal-detachment model for suturing in the region east of the Tanlu Fault. Geology 22, 739–742.

Li, X.H., 2000. Cretaceous magmatism and lithospheric extension in southeast China. Journal of Asian Earth Sciences 18, 293–305.

Lin, G., Zhang, Y.H., Wang, Y.J., Guo, F., Fang, W.M., Yan, Y., 2004. Lithospheric thinning in the North China block: a numerical approach on thermal perturbation and tectonic extension. Geotectonica et Metallogenia 28, 8–14.

Liu, J.M., Ye, J., Xu, J.H., Jiang, N., Ying, H.L., 2001. Preliminary discussion on geodynamic background of Mesozoic gold metallogeny in eastern North China-with examples from eastern Shandong Province. Progress in Geophysics 16, 39–46.

Liu, S., Hu, R.Z., Zhao, J.H., Feng, C.X., 2004. K–Ar Geochronology of Mesozoic mafic dikes in Shandong Province, Eastern China: implications for crustal extension. Acta Geologica Sinica 78, 1207–1213.

Liu, S., Hu, R.Z., Feng, C.X., Zou, H.B., Li, C., Chi, X.G., Peng, J.T., Zhong, H., Qi, L., Qi, Y.Q., Wang, T., 2008a. Cenozoic high Sr/Y volcanic rocks in the Qiangtang terrane, northern Tibet: geochemical and isotopic evidence for the origin of delaminated lower continental melts. Geological Magazine 145 (4), 463–474.

Liu, S., Hu, R.Z., Gao, S., Feng, C.X., Qi, Y.Q., Wang, T., Feng, G.Y., Coulson, I.M., 2008b. U–Pb zircon age, geochemical and Sr–Nd–Pb–Hf isotopic constraints on age and origin of alkaline intrusions and associated mafic dikes from Sulu orogenic belt, Eastern China. Lithos 106, 365–379.

Liu, S., Hu, R.Z., Gao, S., Feng, C.X., Zhong, H., Qi, Y.Q., Wang, T., Qi, L., Feng, G.Y., 2008c. K–Ar Ages and Geochemical + Sr–Nd Isotopic Compositions of Adakitic Volcanic Rocks, Western Shandong Province, Eastern China: foundering of the Lower Continental Crust. International Geological Review 50, 763–779.

Liu, S., Hu, R.Z., Gao, S., Feng, C.X., Qi, L., Zhong, H., Xiao, T.F., Qi, Y.Q., Wang, T., Coulson, I.M., 2008d. Zircon U–Pb geochronology and major, trace elemental and Sr–Nd–Pb isotopic geochemistry of mafic dykes in western Shandong Province, east China: constrains on their petrogenesis and geodynamic significance. Chemical Geology 255, 329–345.

Liu, S., Zou, H.B., Hu, R.Z., Zhao, J.H., Feng, C.X., 2006. Mesozoic mafic dikes from the Shandong Peninsula, North China Craton: Petrogenesis and tectonic implications. Geochemical Journal 40, 181–195.

Liu, Y.S., Gao, S., Kelemen, P.B., Xu, W.L., 2008. Recycled crust controls contrasting source compositions of Mesozoic and Cenozoic basalts in the North China Craton. Geochimica et Cosmochimica Acta 72, 2349–2376.

Lu, Z.G., Tao, K.Y., Xie, J.Y., Xie, D.K., Wang, W.B., Chen, H.N., 1997. Volcanic geology and mineral deposits in the southeast China continent. Geological Publishing House 431, Beijing (in Chinese with English abstract).

Lu, F.X., Zheng, J.P., Li, W.P., Chen, M.H., Cheng, Z.M., 2000. Then main evolution pattern of phanerozoic mantle in the eastern China: the "Mushroom cloud" model. Earth Science Frontiers 7, 97–106 (in Chinese).

Ludwig, K.R., 2003. ISOPLOT 3.0: A Geochronological Toolkit for Microsoft Excel. Berkeley Geochronology Center, Special Publication No. 4.

Lugmair, G.W., Harti, K., 1978. Lunar initial ^{143}Nd/^{144}Nd: differential evolution of the lunar crust and mantle. Earth and Planetary Science Letters 39, 349–357.

Macpherson, C.G., Dreher, S.T., Thirlwall, M.F., 2006. Adakites without slab melting: high pressure differentiation of island arc magma, Mindanao, the Philippines. Earth and Planetary Science Letters 243, 581–593.

Mahoney, J.J., Natland, J.H., White, W.M., Poreda, R., Bloomer, S.H., Fisher, R.L., Baxter, A.N., 1989. Isotopic and geochemical provinces of the western Indian Ocean spreading. Journal of Geophysical Research 94, 4033–4052.

Mahoney, J.J., Frei, R., Tejada, M.L.G., Mo, X.X., Leat, P.T., Nagler, T.P., 1998. Tracing the Indian Ocean mantle domain through time: isotopic results from old west Indian, east Tethyan, and South Pacific seafloor. Journal of Petrology 39, 1285–1306.

Martin, H., 1998. Adakitic magmas: modern analogues of Archaean granitoids. Lithos 46, 411–429.

Martin, H., Smithies, R.H., Rapp, R., Moyen, J.F., Champion, D., 2005. An overview of adakite, tonalite–trondhjemite–granodiorite (TTG), and sanukitoid: relationships and some implications for crustal evolution. Lithos 79, 1–24.

Menzies, M., Xu, Y., Zhang, H., Fan, W., 2007. Integration of geology, geophysics and geochemistry: a key to understanding the North China Craton. Lithos 96 (1–2), 1–21.

Menzies, M.A., Fan, W.M., Zhang, M., 1993. Paleozoic and Cenozoic Lithoprobes and Loss of >120 km of Archean Lithosphere, Sino-Korean Craton, China, Magmatic Processes and Plate Tectonics. Geol Soc Spel Publ., Academic Press, London.

Menzies, M.A., Fan, W.M., Zhang, M., 1993. Paleozoic and cenozoic lithoprobes and the loss of >120 km of Archean lithosphere, Sino-Korean craton, China. In: Prichard, H.M., Alabaster, T., Harris, N.B.W., Neary, C.R. (Eds.), Magmatic Processes and Plate Tectonics, vol. 76. Geol Soc Spec Pub, pp. 71–81.

Middlemost, E.A.A., 1975. Contribution to the nomenclature and classification of volcanic rocks. Geological Magazine 117, 7–51.

Muir, R.J., Weaver, S.D., Bradshaw, J.D., Eby, G.N., Evans, J.A., 1995. Geochemistry of the cretaceous separation point batholith, New Zealand: granitoid magmas formed by melting of mafic lithosphere. Journal of the Geological Society London 152, 689–701.

Münker, C., Pfänder, J.A., Weyer, S., Büchl, A., Kleine, Mezger, T.K., 2003. Evolution of planetary cores and the Earth–Moon system from Nb/Ta systematics. Science 301, 84–87.

Niu, Y.L., 2005. Generation and evolution of basaltic magmas: some basic concepts and a new view on the origin of Mesozoic–Cenozoic basaltic volcanism in Eastern China. Geological Journal of China University 11, 9–46.

Pearce, J.A., Norry, M.J., 1979. Petrogenetic implications of Ti, Zr, Y and Nb variations in volcanic rocks. Contributions to Mineralogy and Petrology 69, 33–47.

Petford, N., Atherton, M., 1996. Na-rich partial melts from newly underplated basaltic crust: the Cordillera Blanca Batholith, Peru. Journal of Petrology 37, 1491–1521.

Prouteau, G., Scaillet, B., Pichavant, M., Pichavant, M., Maury, R.C., 1999. Fluid-present melting of ocean crust in subduction zones. Geology 27, 111–114.

Qi, L., Hu, J., Grégoire, D.C., 2000. Determination of trace elements in granites by inductively coupled plasma mass spectrometry. Talanta 51, 507–513.

Qiu, J.S., Wang, D.Z., Ren, Q.J., Zhang, C.Z., 1994. Physical–chemical conditions for mineralization of the Qibaoshan gold–copper deposit and its metallogeny in Wulian County, Shandong Province. Mineral Resources and Geology 1, 12–18 (in Chinese with English Abstract).

Rapp, R.P., Watson, E.B., 1995. Dehydration melting of metabasalt at 8–32 kbar: implications for continental growth and crust–mantle recycling. Journal of Petrology 36, 891–931.

Rapp, R.P., Shimizu, N., Norman, M.D., 2003. Growth of early continental crust by partial melting of eclogite. Nature 425, 605–609.

Rapp, R.P., Shimizu, N., Norman, M.D., Applegate, G.S., 1999. Reaction between slab-derived melts and peridotite in the mantle wedge: experimental constraints at 38 GPa. Chemical Geology 160, 335–356.

Rapp, R.P., Watson, E.B., Miller, C.F., 1991. Partial melting of amphibolite/eclogite and the origin of Archean trondhjemites and tonalites. Precambrian Research 51, 1–25.

Rapp, R.P., Xiao, L., Shimizu, N., 2002. Experimental constraints on the origin of potassium-rich adakite in east China. Acta Petrologica Sinica 18, 293–311.

Rehkämper, M., Hofmann, A.W., 1997. Recycled ocean crust and sediment in Indian Ocean MORB. Earth and Planetary Science Letters 147, 93–106.

Rudnick, R.L., 1995. Making continental crust. Nature 378, 571–578.

Rudnick, R.L., Gao, S., Ling, W.L., Liu, Y.S., McDonough, W.F., 2004. Petrology and geochemistry of spinel peridotite xenoliths from Hannuoba and Qixia, North China craton. Lithos 77 (1–4), 609–637.

Rudnick, R.L., Fountain, D.M., 1995. Nature and composition of the continental crust: a lower crustal perspective. Reviews of Geophysics 33, 267–309.

Sajona, F.G., Naury, R.C., Pubellire, M., Leterrier, J., Bellon, H., Cotton, J., 2000. Magmatic source enrichment by slab-derived melts in young post-collision setting, central Mindanao (Philippines). Lithos 54, 173–206.

SBGMR (Shandong Bureau of Geology and Mineral Resources), 1995. Map of Regional Geology of Zhigou, Shandong Province (1:50000).

Sen, C., Dunn, T., 1994. Dehydration melting of a basaltic composition amphibolite at 1.5 and 2.0 GPa: implications for the origin of adakites. Contributions to Mineralogy and Petrology 117, 394–409.

Shi, Z.H., Liu, Z.P., Yin, X.H., 1989. Crust thickness (calculated by gravity). In: Ma, X.Y. (Ed.), Lithosphere dynamics atlas of China. Seismological Publishing House, Beijing, China.

Shimoda, G., Tatsumi, Y., Nohda, S., Ishizaka, K., Jahn, B.M., 1998. Setouchi high-Mg andesites revisited: Geochemical evidence for melting of subducting sediments. Earth and Planetary Science Letters 160, 479–492.

Skjerlie, K.P., Patiño Douce, A.E., 2002. The fluid-absent partial melting of a zoisite-bearing quartz eclogite from 1.0 to 3.2 GPa: implications for melting in thickened continental crust and for subduction-zone processes. Journal of Petrology 43, 291–314.

Sobolev, A.V., Hofmann, A.W., Kuzmin, D.V., Yaxley, G.M., Arndt, N.T., Chung, S.-L., Danyushevsky, L.V., Elliott, T., Frey, F.A., Garcia, M.O., Gurenko, A.A., Kamenetsky, V.S., Kerr, A.C., Krivolutskaya, N.A., Matvienkov, V.V., Nikogosian, I.K., Rocholl, A., Sigurdsson, I.A., Sushchevskaya, N.M., Teklay, M., 2007. The amount of recycled crust in sources of mantle-derived melts. Science 316 (5823), 412–417.

Sobolev, A.V., Hofmann, A.W., Sobolev, S.V., Nikogosian, I.K., 2005. An olivine-free mantle source of Hawaiian shield basalts. Nature 434, 590–597.

SPFGSME (Shandong Province of the Fourthly Geological Survey and Mineral Exploration), 2003. Region Geology of Shandong Province. Ji'nan. Publishing House of the Map of Shandong Province, pp. 1–965.

Steiger, R.H., Jäger, E., 1977. Subcommission on geochronology; convention on the use of decay constants in geochronology and cosmochronology. Earth and Planetary Science Letters 36, 359–362.

Stern, C.R., Kilian, R., 1996. Role of the subducted slab, mantle wedge and continental crust in the generation of adakites from the Austral volcanic zone. Contributions to Mineralogy and Petrology 123, 263–281.

Stern, R.A., Hanson, G.N., 1991. Archean high-Mg granodiorite: a derivative of light rare earth element enriched monzodiorite of mantle origin. Journal of Petrology 32, 201–238.

Stracke, A., Bizimis, M., Salters, V.J.M., 2003. Recycling oceanic crust: quantitative constraints. Geochemical and Geophysics Geosystem 4 (3), 8003. doi:10.1029/2001GC000223.

Sun, S.S., McDonough, W.F., 1989. Chemical and isotopic systematics of oceanic basalts: implications for mantle composition and processes. In: Norry, M.J., Saunders, A.D. (Eds.), Magmatism in the Ocean Basins. Geological Society Special Publication, London, pp. 313–345.

Tatsumi, Y., 1986. Chemical characteristics of fluid phase released from a subduction lithosphere and origin of arc magma: evidence from high-pressure experiments and natural rocks. Journal of Volcanology and Geothermal Research 29, 293–309.

Tribuzio, R., Thirlwall, M.F., Vannucci, R., Matthew, F., 2004. Origin of the gabbro–peridotite association from the Northern Apennine Ophiolites (Italy). Journal of Petrology 45, 1109–1124.

Wang, Q., 2000. The study pertaining to rock probes of the dynamics of the deep earth: examples of adakitic and alkali-rich igneous rocks in Southeast China (Including the Dabie Orogen). Postdoctoral Research Report of the Guangzhou Institute of Geochemistry, Chinese Academy of Sciences, pp. 69–108 (in Chinese with English abstract).

Wang, Q., McDermott, F., Xu, J.F., Bellon, H., Zhu, Y.T., 2005. Cenozoic K-rich adakitic volcanic rocks in the Hohxil area, northern Tibet: lower-crustal melting in an intracontinental setting. Geology 33, 465–468.

Wang, Q., Wyman, D.A., Xu, J.F., Jian, P., Zhao, Z.H., Li, C.F., Xu, W., Ma, J.L., He, B., 2007. Early Cretaceous adakitic granites in the Northern Dabie Complex, central China: implications for partial melting and delamination of thickened lower crust. Geochimica et Cosmochimica Acta 71, 2609–2636.

Wang, Q., Wyman, D.A., Xu, J.F., Zhao, Z.H., Jian, P., Xiong, X.L., Bao, Z.W., Li, C.F., Bai, Z.H., 2006b. Petrogenesis of Cretaceous adakitic and shoshonitic igneous rocks in the Luzong area, Anhui Province (eastern China): implications for geodynamics and Cu–Au mineralization. Lithos 89, 424–446.

Wang, Q., Xu, J.F., Zhao, Z.H., Bao, Z.W., Xu, W., Xiong, X.L., 2004. Cretaceous high-potassium intrusive rocks in the Yueshan–Hongzhen area of east China: adakites in an extensional tectonic regime within a continent. Geochemical Journal 38, 417–434.

Wang, Q., Xu, J.F., Zhao, Z.H., Xiong, X.L., Bao, Z.W., 2003b. Petrogenesis of the Mesozoic intrusive rocks in the Tongling area, Anhui Province, China and their constraint to geodynamics process. Science in China, Series D 46, 801–815.

Wang, Q., Xu, J.F., Jian, P., Bao, Z.W., Zhao, Z.H., Li, C.F., Xiong, X.L., Ma, J.L., 2006a. Petrogenesis of adakitic porphyries in an extensional tectonic setting, Dexing, South China: implications for the genesis of porphyry copper mineralization. Journal of Petrology 47, 119–147.

Wang, Q., Zhao, Z.H., Xu, J.F., Li, X.H., Bao, Z.W., Xiong, X.L., 2003a. Petrogenesis and metallogenesis of the Yanshanian adakite-like rocks in the Eastern Yangtze Block. Science in China, Series D 46 (Suppl.), 164–176.

Wang, Y., 1991. Geological characteristics and origin of Qibaoshan gold deposit in Shandong Provnice. Geological Review 37 (4), 329–337 (in Chinese with English abstract).

White, W.M., Hofmann, A.W., Puchelt, H., 1987. Isotope geochemistry of Pacific mid-ocean ridge basalt. Journal of Geophysics Research 92, 4881–4893.

Wilde, S.A., Zhou, X.H., Nemchin, A.A., Sun, M., 2003. Mesozoic crust-mantle interaction beneath the North China craton: a consequence of the dispersal of Gondwanaland and accretion of Asia. Geology 31, 817–820.

Wu, F.Y., Walker, R.J., Ren, X.W., Sun, D.Y., Zhou, X.H., 2003. Osmium isotopic constraints on the age of lithospheric mantle beneath northeastern China. Chemical Geology 196, 107–129.

Wu, F.Y., Walker, R.J., Yang, Y.-H., Yuan, H.-L., Yang, J.-H., 2006. The chemical-temporal evolution of lithospheric mantle underlying the North China Craton. Geochimica et Cosmochimica Acta 70 (19), 5013–5034.

Wu, F.Y., Lin, J.Q., Wilde, S.A., Zhang, X.O., Yang, J.H., 2005. Nature and significance of the Early Cretaceous giant igneous event in eastern China. Earth Planetary Science Letters 233, 103–119.

Wu, G.Y., Jiang, C.H., Ma, L., Ding, X.K., 2002. Occurring of the east china Yanshanian plateau and its inspiration to mineral and petroleum resources evolution. Petroleum Geology and Experiment 24 (1), 3–12 (in Chinese with English Abstract).

Wu, Y.B., Zheng, Y.F., Zhou, J.B., 2004. Neoproterozoic granitoid in Northwest Sulu and its bearing on the North-South China blocks boundary in east China. Geophysics Research Letters 31, L07616.

Xie, Z., Li, Q.Z., Gao, T.S., 2006. Comment on ‘‘Petrogenesis of post-orogenic syenites in the Sulu orogenic belt, east China: Geochronological, geochemical and Nd–Sr isotopic evidence" by Yang et al. Chemical Geology 235, 191–194.

Xiong, X.L., Adam, J., Green, T.H., 2005. Rutile stability and rutile/melt HFSE partitioning during partial melting of hydrous basalt: implications for TTG genesis. Chemical Geology 218, 339–359.

Xiong, X.L., Li, X.H., Xu, J.F., Li, W.X., Zhao, Z.H., Wang, Q., 2003. Extremely high-Na adakite-like magmas derived from alkali-rich basaltic underplate: the Late Cretaceous Zhantang andesites in the Huichang Basin, SE China. Geochemical Journal 37, 233–252.

Xu, J.F., Castillo, P.R., 2004. Geochemical and Nd–Pb isotopic characteristics of the Tethyan asthenosphere: implications for the origin of the Indian Ocean mantle domain. Tectonophysics 393, 9–27.

Xu, J.F., Castillo, P.R., Chen, F.R., Niu, H.C., Yu, X.Y., Zhen, Z.P., 2003. Geochemistry of late Paleozoic mafic igneous rocks from the Kuerti area, Xinjiang, northwest China: implications for backarc mantle evolution. Chemical Geology 193, 137–154.

Xu, J.F., Shinjo, R., Defant, M.J., Wang, Q.A., Rapp, R.P., 2002. Origin of Mesozoic adakitic intrusive rocks in the Ningzhen area of east China: partial melting of delaminated lower continental crust? Geology 30, 1111–1114.

Xu, J.R., Zhao, Z.X., 2004. Structure characteristics of crustal root of mountain beneath the Sulu orogenic belt. Acta Petrologica Sinica 20 (1), 149–156.

Xu, W.L., Wang, Q.H., Wang, D.Y., Guo, J.H., Pei, F.P., 2006. Mesozoicadakitic rocks from the Xuzhou–Suzhou area, eastern China: evidence for partial melting of delaminated lower continental crust. Journal of Asian Earth Sciences 27, 454–464.

Xu, X., O'Reilly, S.Y., Griffin, W.L., Zhou, X., 2000. Genesis of youth lithospheric mantle in southeastern China: a LAM-ICPMS trace element study. Journal of Petrology 41, 111–148.

Xu, Y.G., 2001. Thermo-tectonic destruction of the Archaean lithospheric keel beneath the Sino-Korean craton in China: evidence, timing and mechanism. Physics and Chemistry of the Earth 26, 747–757.

Yan, J., Chen, J.F., Yu, G., Qian, H., Zhou, T.X., 2003. Pb isotopic characteristics of Late Mesozoic mafic rocks from the Lower Yangtze Region: evidence for enriched mantle. Journal of China University of Geosciences 9, 195–206 (in Chinese).

Yang, J.H., Chung, S.L., Wilde, S.A., Wu, F.Y., Chu, M.F., Lo, C.H., Fan, H.R., 2005. Petrogenesis of post-orogenic syenites in the Sulu Orogenic Belt, East China: geochronological, geochemical and Nd–Sr isotopic evidence. Chemical Geology 214, 99–125.

Yang, J.H., Chung, S.L., Zhai, M.G., Zhou, X.H., 2004. Geochemical and Sr–Nd–Pb isotopic compositions of mafic dikes from the Jiaodong Peninsula, China: evidence for vein-plus-peridotite melting in the lithospheric mantle. Lithos 73, 145–160.

Yang, J.H., Zhou, X.H., 2001. Rb–Sr, Sm–Nd, and Pb isotope systematics of pyrite: implications for the age and genesis of lode gold deposits. Geology 29 (8), 711–714.

Yang, L.Q., Deng, J., Ge, L.S., Wang, Q.F., Zhang, D., Gao, B.F., Jiang, S.Q., Xu, H., 2006. Summarization on the ages and genesis of the gold deposits in Jiaodong. Progress in Natural Science 16, 791–801.

Yaxley, G.M., Green, D.H., 1998. Reactions between eclogite and peridotite: mantle refertilisation by subduction of oceanic crust. Schweizerishe. Mineralogische and Petrographische Mitteilungen 78, 243–255.

Yaxley, G.M., 2000. Experimental study of the phase and melting relations of homogeneous basalt plus peridotite mixtures and implications for the petrogenesis of flood basalts. Contributions to Mineralogy Petrology 139, 326–338.

Yuan, H.L., Gao, S., Liu, X.M., Li, H.M., Gunther, D., Wu, F.Y., 2004. Accurate U–Pb age and trace element determinations of zircon by laser ablation-inductively coupled plasma mass spectrometry. Geostand Newslett 28, 353–370.

Zandt, G., Gilbert, H., Owens, T.J., Ducea, M., Saleeby, J., Jones, C.H., 2004. Active foundering of a continental arc root beneath the southern Sierra Nevada in California. Nature 431, 41–46.

Zhai, M.G., Yang, J.H., Liu, W.J., 2001. Large clusters of gold deposits and large-scale metallogenesis in the Jiaodong Peninsula. Eastern China 2001 44 (8), 758–768.

Zhang, H.F., Sun, M., Zhou, M.F., Fan, W.M., Zhou, X.H., Zhai, M.G., 2004. Highly heterogeneous Late Mesozoic lithospheric mantle beneath the North China Craton: evidence from Sr–Nd–Pb isotopic systematics of mafic igneous rocks. Geological Magazine 141 (1), 55–62.

Zhang, H.F., Ying, J.F., Shimoda, G., Kita, N.T., Morishita, Y., Shao, J.-A., Tang, Y.-J., 2007. Importance of melt circulation and crust-mantle interaction in the lithospheric evolution beneath the North China Craton: evidence from Mesozoic basalt-borne clinopyroxene xenocrysts and pyroxenite xenoliths. Lithos 96, 67–89.

Zhang, H.F., Li, S.R., Zhai, M.G., Guo, J.H., 2006. Crust uplift and its applications in the Jiaodong Peninsula eastern China. Acta Petrologica Sinica 22 (2), 285–295.

Zhang, Q., Qian, Q., Wang, E.C., Wang, Y., Zhao, T.P., Hao, J., 2001. Existence of the East China Plateau in the mid-late Yanshan period: implications from adakites. Scientia Geologica Sinica 36, 248–255 (in Chinese with English Abstract).

Zhao, G., Wang, D., Cao, Q., 1997. Geochemical features and petrogenesis of Laoshan Granite in east Shandong Province. Geological Journal of China Universities 3, 1–15 (in Chinese with English Abstract).

Zhao, Z.F., Zheng, Y.F., Wei, C.S., Wu, Y.B., 2007. Post-collisional granitoids from the Dabie orogen in China: Zircon U–Pb age, element and O isotope evidence for recycling of subducted continental crust. Lithos 93, 248–272.

Zheng, J.P., Lu, F.X., 1999. Mantle xenoliths from kimberlites, Shandong and Liaoning: paleozoic mantle character and its heterogeneity. Acta Petrology Sinica 15, 65–74 (in Chinese).

Zheng, Y.F., Wang, Z.R., Li, S.G., Zhao, Z.F., 2002. Oxygen isotope equilibrium between eclogite minerals and its constraints on mineral Sm–Nd chronometer. Geochimica et Cosmochimica Acta 66, 625–634.

Zheng, Y.F., Zhou, J.B., Wu, Y.B., Xie, Z., 2005. Low-grade metamorphic rocks in the Dabie-Sulu orogenic belt: a passive margin accretionary wedge deformed during continent subduction. International Geological Review 47, 851–871.

Zhou, J.B., Wilde, S.A., Zhao, G.C., Zhang, X.Z., Zheng, C.Q., Jin, W., Cheng, H., 2008. SHRIMP U–Pb zircon dating of the Wulian complex: defining the boundary between the North and South China Cratons in the Sulu Orogenic Belt, China. Precambrian Research 162, 559–572.

Zhou, J.B., Zheng, Y.F., Zhao, Z.F., 2003. Zircon U–Pb Dating on Mesozoic Granitoids at Wulian, Shangdong Province. Geological Journal of China Universities 9 (2), :185–194.

Zhou, T.H., Lu, G.X., 2000. Tectonics, granitoids and Mesozoic gold deposits in East Shandong, China. Ore Geology Reviews 16, 71–90.

Zi, F., He, G.Y., Dai, S.Q., Xu, W., 2007. Liguo early cretaceous high-Mg adakitic intrusive rocks in the Xuzhou region: petrogenesis fro geodynamics and mineralization. Acta Petrologica Sinica 23 (11), 2857–2868.

Zou, H.B., Zindler, A., Xu, X.S., Qi, Q., 2000. Major, trace element, and Nd, Sr and Pb isotope studies of Cenozoic basalts in SE China: mantle sources, regional variations and tectonic significance. Chemical Geology 171, 33–47.